

ALMA MATER STUDIORUM · UNIVERSITY OF BOLOGNA

School of Science
Department of Physics and Astronomy
Master Degree in Physics

DECONFINED QUANTUM CRITICALITY

Supervisor:
Prof. Elisa Ercolessi

Submitted by:
Umberto Di Laudo

Academic Year 2020/2021

Abstract

In this work it is studied a type of quantum phase transitions beyond the Landau-Ginzburg-Wilson (LGW) paradigm. In particular it is described a second order transition between the Néel and the Valence Bond Solid (VBS) states for a two dimensional quantum square lattice with antiferromagnetic interactions. The natural description of this critical theory is not given in terms of the order parameter, but in terms of an emergent gauge field which mediates interactions between "fractional" particles. These particles are confined on either sides of the transition, while they emerge at the critical point, that is thus called "deconfined". This critical theory corresponds to that of a 3D classical $O(3)$ model with monopoles suppressed. In the second part of this work, this model is numerically simulated by using Monte Carlo methods, and its critical exponents are obtained.

Abstract

In questo lavoro è mostrato un tipo di transizione di fase quantistica che non può essere descritto dalla teoria di Landau-Ginzburg-Wilson (LGW). Nello specifico viene descritta una transizione quantistica del secondo ordine tra uno stato di Néel e uno stato Valence Bond Solid (VBS) per un sistema antiferromagnetico bidimensionale su un reticolo quadrato. Tale teoria non viene descritta in termini di un parametro d'ordine, bensì in termini di un nuovo campo di gauge che è caratteristico solo del punto critico e media l'interazione tra particelle frazionarie. Queste particelle sono assenti in entrambe le fasi ed emergono solamente nel punto critico. Questa teoria critica corrisponde a quella di un modello di Heisenberg classico tridimensionale con la soppressione di monopoli. Nella seconda parte del lavoro, tramite il metodo Monte Carlo, questo modello è stato studiato numericamente e se ne sono calcolati gli esponenti critici.

Contents

Introduction	3
1 Quantum antiferromagnets	6
1.1 LGW transitions	6
1.2 Coupled dimer antiferromagnet	9
2 The deconfined transitions	12
2.1 Néel-VBS	12
2.1.1 Topology	14
2.2 CP^1 representation	17
2.3 Easy-plane anisotropy	18
2.4 Isotropic case	23
2.5 Physical properties	24
3 Monte Carlo Simulations	27
3.1 Classical Heisenberg model	28
3.2 Topological charge	33
3.3 Hedgehog Suppression	36
3.3.1 Close pairs	36
3.3.2 Isolated pairs	41
4 Conclusions	43
A Non linear sigma model	45
A.1 Spin coherent states	45
A.2 Path-integral	47
A.3 Haldane's Mapping	49

B Topological term	52
B.1 Without Berry phase	53
B.2 With Berry phase	54
C Monte Carlo tools	57
C.1 Statistical error	59

Introduction

The theory of phase transitions is crucial in the study of modern statistical mechanics and condensed matter theory. An important element in this context is the *order parameter*, that expresses the different symmetries of the phases on either parts of critical point. If the transition is continuous *i.e.* of the second order, the theory shows many physical quantities with universal singular behaviour. Ginzburg and Landau [14] showed how these universal singularities are associated with the long wavelength low energy fluctuations of the order parameter. Together with to the sophisticated renormalization group theory of Wilson [35], it forms the so called Landau-Ginzburg-Wilson (LGW) paradigm. This is very important for understanding critical singularity in different contexts. According to it effective theories in which all modes but the order parameters are eliminated can be used in order to determine critical properties.

At $T = 0$, thermal fluctuations are suppressed, but quantum fluctuations can still play a fundamental role. As the coupling parameters in a Hamiltonian vary, they can become dominant and drive a *quantum phase transitions*. It is believed that many properties of correlated materials are due to the competition between different ground states. Examples are the cuprate high T_c superconductors and the heavy fermion materials [30]. The LGW paradigm was adapted to these quantum critical phenomena too.

Evidences of the failure of the LGW paradigm appear already for the classical two dimensional XY model with the *BKT* transition between bound vortex-antivortex pairs to unpaired vortex and antivortex [4]. Moreover in the last few years the number of models that break the LGW paradigm has increased. In general they correspond to situations in which the topological structure of the model plays a crucial role, as in the case of the quantum spin chains studied by Haldane [8]. Numerical calculations [30] showed a second order transition between two states with different broken symmetry.

LGW paradigm predict either a first order transition or an intermediate region of coexistence of the two states. There are also many experiments that prove the onset of such phase transitions, such as magnetic long range order in a class of rare-earth intermetallics (heavy fermion metals) [6].

In the first part of this work it is reported a specific transition for a two dimensional $S = 1/2$ quantum square lattice with antiferromagnetic interactions, between two ordered phases: the Néel and the *Valence bond solid* phase that break respectively rotational and translational symmetry. Despite the LGW paradigm predicts a first order transition, it was find out a second order one. A LGW analysis would suggest a formulation of a critical theory in terms of the Néel field \hat{n} and VBS order parameter ψ_{VBS} . The natural description of this theory instead is in terms of a new degree of freedom specific to the critical point. In our case it corresponds to a gauge field that mediates interactions between fractional particles *i.e.* particles that carry fractions of the quantum number of the field. These particles are confined on both side of the transition but they appear naturally at the quantum critical point (QCP). For this reason this is called *deconfined* QCP.

In this framework it is important to look at the topology of the model: smooth configurations of the Néel field \hat{n} admit *skyrmions*. Changes in skyrmions number corresponds to monopole events. A crucial role is played by the Berry phase which makes irrelevant the monopole events (creation of skyrmions) at the QCP. The absence of monopoles leads to a new conserved quantity, the flux of the gauge field, that is related with a symmetry that is not present in the microscopical Hamiltonian. While monopoles are not present at the QCP, they are relevant in paramagnetic phase and leads to a VBS ground state.

This particular behaviour of monopoles, that are thus said *dangerous irrelevant*, ensures the existence of two different correlation lengths ξ and ξ_{VBS} , both diverging at criticality. The first is the "standard" spin-spin correlation length, while the second measures the thickness of the domain wall between two valence bond states and it diverges faster then ξ . The emergence of spinons at the criticality leads to large anomalous dimension of the Néel order.

Due to the irrelevance of monopole at QCP, the critical theory is the same of a $O(3)$ classical Heisenberg model with monopoles suppressed in a cubic lattice. In the second part of this work we use Monte Carlo methods in order to numerically simulate this model. Actually we first simulate a "standard" classical $O(3)$ Heisenberg

system and find out the critical exponents of transition between the ordered and the paramagnetic phase. It is seen that neglecting configurations of spin that contain monopoles, there is no transition at all. On the other hand, the transition is restored by allowing configurations with pairs of monopoles to exist. The critical exponents are very different from that of the "standard" $O(3)$ Heisenberg model.

Chapter 1

Quantum antiferromagnets

In this chapter we are going to talk about quantum antiferromagnets. In particular we will focus on second order quantum transitions of two dimensional systems defined on square lattice. Traditional second order quantum phase transitions are described by the Landau-Ginzburg-Wilson paradigm [14, 35]. Their idea was to describe the critical singularities with long wavelength fluctuations of an order parameter which is able to encode the difference in the order of the two phases on either sides of the critical point.

1.1 LGW transitions

In a LGW framework the antiferromagnetic transition is described by the Néel order parameter φ_α ($\alpha = x, y, z$) that is $\langle \varphi_\alpha \rangle \neq 0$ in the Néel state, while $\langle \varphi_\alpha \rangle = 0$ in the paramagnetic phase.

A simple model that exhibits such transition is given by the $O(n)$ quantum rotors. In this model we have a second order phase transition between an ordered phase which breaks the $O(n)$ symmetry, and a disordered phase which preserves the symmetry of the microscopical Hamiltonian. Another example of transition belonging to the same universality class, is the spin 1/2 quantum Heisenberg spins on a bipartite lattice that we will consider in the next section.

We specialize to the case of $n = 3$. The Hamiltonian of the model is [27, 31]

$$H = g \sum_r \frac{\vec{L}_r^2}{2} - \frac{1}{g} \sum_{\langle rr' \rangle} \hat{n}_r \cdot \hat{n}_{r'} \quad (1.1.1)$$

Here \hat{n}_r is a three dimensional vector such that $\hat{n}_r^2 = 1$. As usual r labels the position of the square lattice sites. Each rotor has an associated momentum \hat{p}_r that is orthogonal to the S_2 sphere on which \hat{n}_r lies, that appears in the Hamiltonian via the rotor angular momentum:

$$L_\alpha = \frac{1}{2} \epsilon_{\alpha\beta\gamma} (n_\beta p_\gamma - n_\gamma p_\beta) \quad (1.1.2)$$

where the index α, β and γ label the three components of the vector and $\epsilon_{\alpha\beta\gamma}$ is the totally antisymmetric tensor. The Hamiltonian is manifestly invariant under any rotation, admitting an $O(3)$ symmetry.

It is clear that for small values of the coupling constant g , the second term dominates and we obtain an ordered ground state with

$$\langle \hat{n} \rangle \neq 0 \quad (1.1.3)$$

The $O(3)$ symmetry is spontaneously broken down to $O(2)$, with a ground state corresponding to a uniform vector \hat{n} while the low energy excitations are two *spin waves* [31] with linear dispersion. On the other hand, for large g , it is the first term that is relevant and we have a paramagnetic ground state with $\langle \hat{n} \rangle = 0$, which preserves the symmetry of the microscopical Hamiltonian. In this case the low energy excitations are gapped and correspond to a massive triplet of spin-1 bosons [31].

As it is described in Appendix A, a suitable continuum theory for this kind of model in $(2 + 1)$ dimensions, is given by the action of the Non Linear Sigma Model (NL σ M) which, in the Euclidean version, reads as:

$$S_{NL\sigma M} = \int d^2x d\tau \frac{1}{2g} \left[(\partial_x \hat{n})^2 + (\partial_y \hat{n})^2 + \frac{1}{c^2} (\partial_\tau \hat{n})^2 \right] \quad (1.1.4)$$

This model gives linear equations of motion, the non-linearity being encoded in the condition $|\hat{n}| = 1$. Like in the discrete case one finds that for $g < g_c$ there is an ordered Nèel phase with spin waves excitations and for $g > g_c$ a disordered phase with a non-zero energy gap and a triplet of excitations, that are called *triplon*.

It is very useful to consider a *soft-spin* version of this theory is in the same universality class and whose action is given by:

$$\mathcal{S}_\varphi = \int d^2r d\tau \left[\frac{1}{2} (\partial_\tau \varphi_\alpha)^2 + c^2 (\partial_x \varphi_\alpha)^2 + c^2 (\partial_y \varphi_\alpha)^2 + s \varphi_\alpha^2 + \frac{u}{24} (\varphi_\alpha^2)^2 \right] \quad (1.1.5)$$

where one has to vary the value of s in order to get the quantum critical point. Here φ_α are the component of the vector $\vec{\varphi} \sim \hat{n}$. The importance of looking at this soft-spin version is the fact that this theory corresponds to the well known classical $O(3)$ invariant Heisenberg ferromagnet and the Curie transition maps onto the quantum critical point. Because of this mapping we can deduce some useful things of the underlined quantum transition. The first thing to notice is that there is a single diverging length [31], so it is natural to associate it in the paramagnetic phase with the spin correlation length. There is also a vanishing energy scale that on the paramagnetic side is taken as the gap of the triplon excitations. The spin gap of the paramagnet goes as $\Delta \sim (g - g_c)^{z\nu}$, where $z = 1$, due to the relativistic invariance of the \mathcal{S}_φ theory. In the next chapter we will study numerically this kind of transition showing that the exponent ν is about 0.705.

Another important aspect can be deduced by looking at the spin correlation the Curie transition at $g = g_c$: it is known [17] that it decays as $\sim 1/p^{2-\eta}$, where modulus of p is the three momentum and η is the anomalous dimension. At the quantum critical point $g = g_c$ we can probe this relation by looking at the dynamic susceptibility, which is related to the Fourier transform of the correlations:

$$\chi_\varphi(k, \omega) \sim \frac{1}{(c^2 k^2 - \omega^2)^{1-\eta/2}} \quad (1.1.6)$$

where we have analytically continued the expression for p from its p_z dependence in the third classical dimension to the real frequency ω . Its imaginary part is given by:

$$Im\chi_\varphi(k, \omega) \sim sgn(\omega) \sin\left(\frac{\pi\eta}{2}\right) \frac{\theta(|\omega| - c|k|)}{(\omega^2 - c^2 k^2)^{1-\eta/2}} \quad (1.1.7)$$

which, as it should be, contains no quasiparticle delta function at the quantum critical point.

If we move in the paramagnetic phase a gap Δ opens and the imaginary part of χ_φ takes the form

$$Im\chi_\varphi(k, \omega) \sim \frac{Z}{\Delta} \delta(\omega - \Delta - O(k^2)) \quad (1.1.8)$$

where Z is the quasiparticle residue.

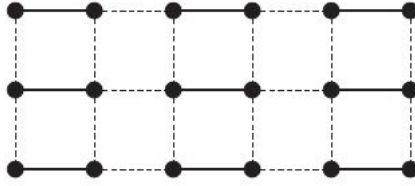


Figure 1.1: The coupled dimer antiferromagnet. The full lines correspond to the \mathcal{A} links while the dashed lines to the \mathcal{B} ones. From [31].

1.2 Coupled dimer antiferromagnet

The kind of transition described in the above section can be seen also in a two dimensional spin-1/2 quantum antiferromagnet, by looking at this Hamiltonian [31]:

$$H_d = J \sum_{\langle ij \rangle \in \mathcal{A}} \vec{S}_i \cdot \vec{S}_j + \frac{1}{g} J \sum_{\langle ij \rangle \in \mathcal{B}} \vec{S}_i \cdot \vec{S}_j \quad (1.2.1)$$

where $J > 0$ and $g \geq 1$, which is defined on a bipartite lattice, *i.e.* a lattice whose links can be separated into two disjoint sets \mathcal{A} and \mathcal{B} . Fig. 1.1 shows the case of the square lattice, where the full (dashed) links represent the set \mathcal{A} (\mathcal{B}). For $g = 1$ one recovers the usual square lattice.

Senthil [29] shows that this model displays a phase transition that fits with the LGW paradigm. Let us consider this model with a value of g near 1. Exactly at $g = 1$ it is well known [30, 17] that the system has a long range Néel order ground state with $\langle \varphi_\alpha(x_j) \rangle \neq 0$ where

$$\varphi_\alpha(x_j) = \eta_j S_{j\alpha} \quad (\alpha = x, y, z) \quad (1.2.2)$$

x_j is the position on the lattice and $\eta_j = e^{i\vec{K} \cdot \vec{x}_j} = \pm 1$, with $\vec{K} = (\pi, \pi)$. We expect that this long-range order remains also for sufficiently small value of $g < g_c$. In this phase there are two spin waves excitations [31, 27], that are spacial deformations in the orientation of $\langle \varphi_\alpha \rangle$ [27]. The energy of these excitations is given by

$$\epsilon_k = (c_x^2 k_x^2 + c_y^2 k_y^2)^{1/2} \quad (1.2.3)$$

where $\vec{k} = (k_x, k_y)$ is the wave vector of the spin waves and c_x and c_y denote the spin waves velocities in the two spacial directions.

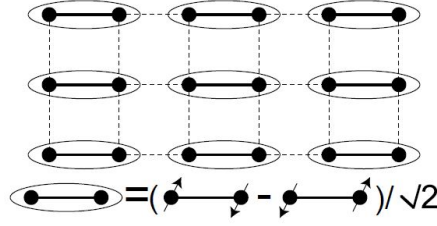


Figure 1.2: Ground state of the Hamiltonian (1.2.1) with $g \rightarrow \infty$. The ovals represent singlet valence bond pairs. From [31].

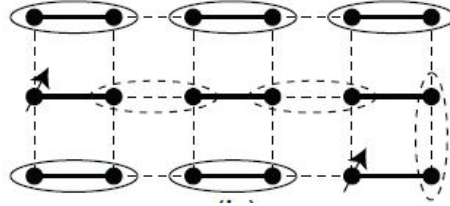


Figure 1.3: Fission of $S = 1$ excitation into two $S = 1/2$ spinons. The dashed circles are valence bonds. From [31]

Consider now big values of $g > g_c$. If we take the extreme case of $g = \infty$ what we have is a Hamiltonian with a set of completely decoupled dimers. The spins in each dimer form a valence bond singlet [8]

$$|(ij)\rangle = \frac{1}{\sqrt{2}}(|\uparrow_i \downarrow_j\rangle - |\downarrow_i \uparrow_j\rangle) \quad (1.2.4)$$

that preserves each symmetry of H_d . This ground state is depicted in Fig. 1.2. In this case the excitations [27] correspond to the breaking of one valence bond singlet that becomes a three-fold degenerate state with total spin $S = 1$. When $g = \infty$ the excitation is localized, instead with $g > g_c$ but still a finite value, it can move from site to site[31]. In this case we can consider it as a triplet quasiparticle excitation usually called *triplon*. In the LGW language this is a quantum of oscillation of φ_α around $\varphi_\alpha = 0$. Its energy is given by [31]

$$\epsilon_k = \Delta + \frac{c_x^2 k_x^2 + c_y^2 k_y^2}{2\Delta} \quad (1.2.5)$$

This $S = 1$ triplon cannot fission into a couple of $S = 1/2$ spinons. Indeed if a situation as described in Fig. 1.3 appears, *i.e.* in which two spinons are connected

by a "string" of valence bonds, the confinement length remains finite also at quantum critical point. This means that the existence of these spinons are a non-universal lattice scale effect and it is not related to the fluctuations that govern the universal critical properties. We will see that the situation is very different for the *deconfined critical point*, where spinons play a very important role.

For this *dimerized* system it is found [30, 31] a transition between the states described above at $g = g_c$, with $1/g_c = 0.52337$ [31]. This transition can be studied using the LGW procedure. We can consider the order parameter φ_α and write the most general effective action that preserves all the symmetries of the Hamiltonian H_d . This φ^4 field theory of Eq. (1.1.5) and all the consideration done in the above section still apply.

Chapter 2

The deconfined transitions

In this chapter we are going to talk about an unusual continuum quantum transition of a two dimensional quantum antiferromagnet [13, 34] giving a piece of evidence of the failure of the LGW paradigm [29]. In fact it was shown that there are transitions that do not fit into this theory. These kinds of processes are not described in terms of the usual order parameter, but in terms of new degrees of freedom that appear only at the critical point, that takes the name of "*deconfined quantum critical point*".

2.1 Néel-VBS

In contrast with the "traditional" transition described in the previous chapter, we now focus on that critical points that does not fit with the LGW approach. An example of this new critical points is the transition between the Néel and the *Valence Bond Solid (VBS)* states.

Consider for example a quantum system of spin=1/2 on two dimensional square lattice:

$$H = J \sum_{\langle rr' \rangle} \vec{S}_r \cdot \vec{S}_{r'} + \dots \quad (2.1.1)$$

where the ellipses represent others short range interactions (controlled by the term g , such as the term appearing in the (2.1.6)) that preserve the symmetry. As before, the interactions are assumed to be antiferromagnetic *i.e.* $J > 0$.

It is useful to define the *Néel vector* \vec{N}_r that describes the staggered magnetization

$$\vec{S}_r = (-1)^{x+y} \vec{N}_r \quad (2.1.2)$$

The Néel state has $\langle \vec{N}_r \rangle \neq 0$, where \vec{N}_r is assumed to be slowly varying on the lattice scale. This ground state clearly breaks spin rotational symmetry.

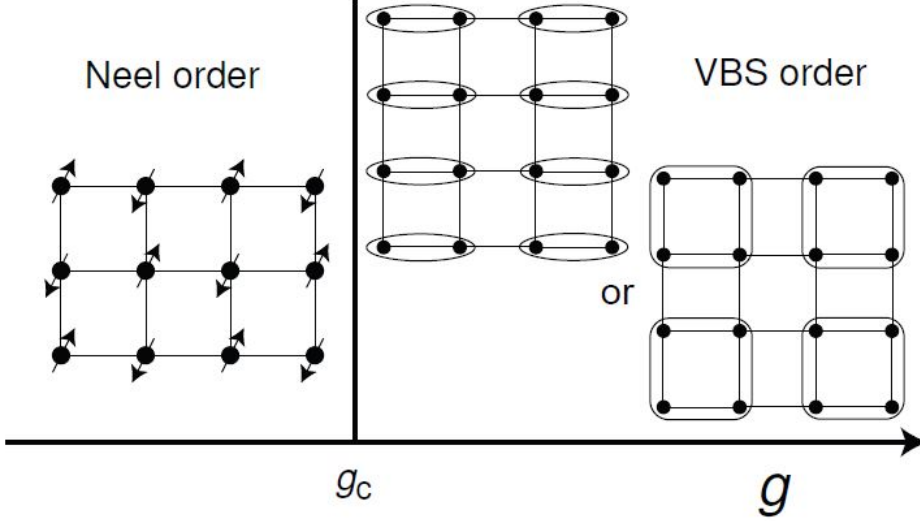


Figure 2.1: Ground states of $S=1/2$ square lattice. The coupling g is the strength of quantum spin fluctuation and controls the short-range exchange interactions that are contained in the ellipses of (2.1.1). It appears in Eq. (2.1.6). For $g > g_c$ there is a VBS state with either columnar (left) or plaquette (right) order. The VBS configurations are similar to that in Fig. 1.1 of the previous section. However here, because of the absence of the dimerization in the starting Hamiltonian (in (2.1.1) all bonds are equivalent) there is spontaneous VBS order with a four-fold degenerate ground state. From [31]

However, it is well known that paramagnetic ground states with $\langle \vec{S}_r \rangle = 0$ are possible. As it is discussed in the Appendix B, a particular state of this kind is the "Valence Bond Solid" (VBS) state that can have "columnar" or "plaquette" order. The VBS state is described by the order parameter ψ_{VBS} [30], which is defined as

$$\langle \vec{S}_r \cdot \vec{S}_{r+x} \rangle \sim \text{Re}[\psi_{VBS}](-1)^x \quad (2.1.3)$$

$$\langle \vec{S}_r \cdot \vec{S}_{r+y} \rangle \sim \text{Im}[\psi_{VBS}](-1)^y \quad (2.1.4)$$

This VBS state clearly breaks lattice translational symmetry. Consider now a transition between this two ordered phases (Néel and VBS): LGW paradigm predicts either a first order transition or passage through an intermediate disordered state. However it will be shown in next sections that a generic second order phase transition between Néel and VBS state is possible which it is natural described in terms of spin 1/2 spinons or CP^1 fields z_α ($\alpha = 1, 2$).

The Néel order parameter is related to the z_α field through:

$$\vec{N} \sim z^\dagger \vec{\sigma} z \quad (2.1.5)$$

2.1.1 Topology

As discussed in Appendix A, in the Néel phase or close to it, the long distance fluctuations of the Néel order parameter are captured by the quantum $O(3)$ Non-Linear Sigma Model (NL σ M) with the euclidian action:

$$\mathcal{S}_n = \frac{1}{2g} \int d\tau \int d^2r \left[\frac{1}{c^2} \left(\frac{\partial \hat{n}}{\partial \tau} \right)^2 + (\nabla_r \hat{n})^2 \right] + iS \sum_r (-1)^r \mathcal{A}_r \quad (2.1.6)$$

where $r = (x, y)$, τ is the imaginary time, and $\hat{n}_r = \frac{\vec{N}_r}{|\vec{N}|}$. The second term is the Berry phase of all the spins and \mathcal{A}_r is the area enclosed by the path mapped out by the time evolution of the vector \hat{n}_r on the surface of a unit sphere. This term is not important in the Néel phase [5] but it plays a crucial role in the paramagnetic one [26].

At low but finite energy, smooth configurations of the Néel vector admit topological texture known as *skyrmions* (see also Appendix B). An example of skyrmion is illustrated in Fig. 2.2. The total *skyrmion number* is a topological number Q defined as

$$Q = \frac{1}{4\pi} \int d^2r \hat{n} \cdot \partial_x \hat{n} \times \partial_y \hat{n} \quad (2.1.7)$$

For smooth configurations, the sum over Berry phases vanishes even if it contains skyrmions [29]. In this case the skyrmion number Q is conserved in time. However in principle this model is defined on the lattice and processes in which Q changes are allowed [9]. These events are characterized by the presence of monopole singularities

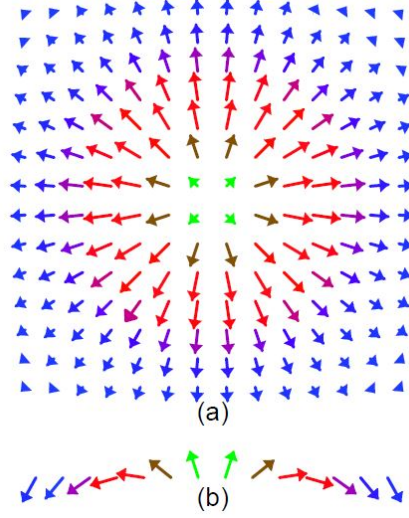


Figure 2.2: A skyrmion configuration of three dimensional vector $\hat{n}(r) = (n_x, n_y, n_z)$. Panel (a) shows the vector (n_x, n_y) on the XY plane while (b) shows the vector (n_x, n_z) along a section of (a) on the X axis. From [29]

in the Néel field $\hat{n}(r, \tau)$ in space-time. An example is showed in Fig. 2.3. In presence of such monopole events, the sum of Berry phases gives a non-vanishing result and the total Berry phase associated with each monopole event oscillates on four sublattices of the dual lattice interfering in a destructive way[9]. This implies that all monopole events can be neglected unless they are quadrupled and then the lowest skyrmion number changing event allowed is when $\Delta Q = \pm 4$. All of these considerations are explored in more details in Appendix B.

Notice that the $NL\sigma M$ part of Eq. (2.1.6) is the continuum limit of the action:

$$\mathcal{S}_n = \int d\tau \left(\sum_r \frac{1}{2g} \left(\frac{d\hat{n}_r}{d\tau} \right)^2 - j \sum_{\langle rr' \rangle} \hat{n}_r \cdot \hat{n}_{r'} \right) + iS \sum_r (-1)^r \int d\tau \vec{A}[\hat{n}] \cdot \frac{d\hat{n}}{d\tau} \quad (2.1.8)$$

where \vec{A} is the vector potential of a magnetic monopole at the center of \hat{n} space at each lattice site.

It is now crucial to note that the monopole creation operator v^\dagger , *i.e.* the skyrmion number changing operator, does not transform trivially under square lattice translations and rotations. Under a $\pi/2$ rotation $R_{\pi/2}$ in the counter-clockwise direction about a lattice site, the Berry phase associated with the skyrmion creation event

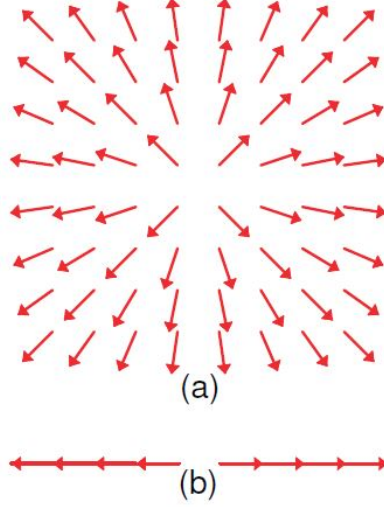


Figure 2.3: An equal time slice of space-time when a monopole event occurs at the origin. In (a) the vector (n_x, n_y) on the XY plane is represented, while in (b) (n_x, n_z) on the X axis is shown. From [29]

changes by $e^{i\pi S}$ [30]. Now if $S = 1/2$, it is clear that [30]

$$R_{\pi/2} : v^\dagger \rightarrow iv^\dagger \quad (2.1.9)$$

Then consider the lattice translation operator $T_{x,y}$ that performs a translation by a unit along the x, y axis:

$$T_x : \hat{n}_r \rightarrow -\hat{n}_{r+x} \quad (2.1.10)$$

$$T_y : \hat{n}_r \rightarrow -\hat{n}_{r+y} \quad (2.1.11)$$

Now it is clear that the skyrmion number Q is odd under this transformation. Then $T_{x,y}$ transforms a skyrmion creation operator in an antiskyrmion creation operator at the translated plaquette. There is also a change due to difference in the Berry phase factor for monopoles on the adjacent plaquettes[30].

$$T_x : v_r^\dagger \rightarrow -iv_{r+x}^\dagger \quad (2.1.12)$$

$$T_y : v_r^\dagger \rightarrow +iv_{r+y}^\dagger \quad (2.1.13)$$

As a consequence, in the paramagnetic phase with $\langle v^\dagger \rangle = \langle v \rangle \neq 0$, $R_{\pi/2}, T_x, T_y$ are broken.

We can note [30] that the lattice transformation properties of v are the same of the VBS order parameters ψ_{VBS} . More precisely we have [30],

$$v \sim e^{-i\pi/4}\psi_{VBS} \quad (2.1.14)$$

Summing over the monopoles event, it can be shown [30] that in paramagnetic phase the Berry phase leads to a condensation of v and v^\dagger and so to VBS order.

Then in principle, the action \mathcal{S}_n of Eq. (2.1.6) can describe both Néel and VBS order.

2.2 CP^1 representation

As we said in the previous section, in order to analyse this model, it is useful to use CP^1 parametrization of the Néel field \hat{n} [1, 8]

$$\hat{n} = z^\dagger \vec{\sigma} z \quad (2.2.1)$$

where $\vec{\sigma}$ is the vector of Pauli matrices and $z(r, \tau) = z(z_1, z_2)$ is a two component spinor. The z_α field are fractionalized spinon field and they satisfy the relation $|z_1|^2 + |z_2|^2 = 1$. It is easy to see that the transformation

$$z \rightarrow e^{i\gamma(r, \tau)} z \quad (2.2.2)$$

leaves the \hat{n} field invariant. This means that the fields z_α have a $U(1)$ gauge redundancy. It is convenient to introduce a $U(1)$ compact gauge field a_μ ($\mu = r, \tau$). It can be shown [29, 20] that the flux of a_μ is exactly the skyrmion number density of \hat{n} :

$$Q = \frac{1}{2\pi} \int d^2x (\partial_x a_y - \partial_y a_x) \quad (2.2.3)$$

Thus a monopole event that changes the flux of a_μ of $\pm 2\pi$ is equivalent to a change of ± 1 of skyrmion number. Because of the compactness of a_μ , the gauge flux is allowed to change by $\pm 2\pi$ and this means a change of skyrmion number *i.e.* it corresponds to a monopole event.

A crucial point of the critical theory between Néel and VBS phases is that the quadrupling of monopole events induced by the Berry phase makes the monopoles *irrelevant* (in renormalization group sense) at the *critical point* $g = g_c$.

This means that we do not have monopole events at the critical point and thus the skyrmion number does not change: there is emergent global topological conservation law that can be explained as an extra global *dual* $U(1)$ symmetry that it is absent in the microscopic hamiltonian. The fact that the flux of a_μ does not change allows us to neglect its *compactness*. Indeed the critical field theory for the Néel-VBS transition is given by writing down the simplest continuum theory of spinons coupled with a non-compact $U(1)$ gauge field a_μ :

$$\mathcal{L}_z = \sum_{a=1}^2 |(\partial_\mu - ia_\mu)z_a|^2 + s|z|^2 + u(|z|^2)^2 + k(\epsilon_{\mu\nu k}\partial_\nu a_k)^2 \quad (2.2.4)$$

where the spinon field z_α are coupled with a *non-compact* gauge field a_μ .

As we can see, there is no monopole terms like

$$\mathcal{L}_{mp} = \sum_{n=1}^{\infty} \lambda_n(r) ([v_{r\tau}]^n + [v_{r\tau}^\dagger]^n) \quad (2.2.5)$$

just because the monopole fugacity λ_4 (that is the only that survives [9, 30]), is *irrelevant* at the critical point. This does not hold away from the critical point in the VBS phase. Indeed, it is known from studies of compact $U(1)$ gauge theory [30], that in paramagnetic phase the fugacity is always relevant and this lead to a proliferation of monopole events and thus to a condensation of $\langle v_{r\tau} \rangle = \langle \psi_{VBS} \rangle \neq 0$ *i.e.* VBS state. As we said before, the conservation of the gauge flux (or the skyrmion number Q), can be understood as a consequence of a global $U(1)$ symmetry in a dual description. Now we realize such construction for easy-plane anisotropy, hence in the case in which spins prefer to lie in the XY plane.

2.3 Easy-plane anisotropy

In the easy-plane the anisotropy tends to orient the spins in a direction orthogonal to the \hat{z} axis. This means the $SU(2)$ spin rotation symmetry reduces to a $U(1)$ symmetry. There is also the time reversal discrete symmetry that transform

$$\vec{S}_r \rightarrow -\vec{S}_r \quad (2.3.1)$$

Combining this with a $U(1)$ rotation of π in the XY plane that restores the x and y component of the spin, this symmetry reduce to a change of the sign of S_z . Thus

this theory can be described by the action (2.1.6) with the addition of a term

$$\mathcal{S}_{ep} = \int d\tau d^2r \omega(n^z)^2 \quad (2.3.2)$$

that favors planar spin configurations.

The classical ground state is clearly a configuration of \hat{n} independent of position and that lies in the XY plane. Topological defects in this case are vortices in the field $n^+ = n_x + in_y$. At the core of this vortices the x and y component of \hat{n} become zero and then, because $|n|^2 = 1$, the field \hat{n} points to the \hat{z} axis. At classical level there are two kind of vortices (*merons*), each one that points in the opposite direction $\pm\hat{z}$. This in principle breaks Z_2 symmetry of the model. At quantum level it is possible [29] to have tunnelling events between the two kind of classical vortex and this restores the Ising-like symmetry.

Let's define the creation operator of each kind of meron as ψ_1^\dagger and ψ_2^\dagger . As we see from Fig. 2.4, each meron can be seen as half a skyrmion: in fact if we take ψ_2 at $\tau \rightarrow -\infty$ and ψ_1 at $\tau \rightarrow +\infty$ this two configurations cannot smoothly deformed one into each other and we have to put a singularity at the origin of the space-time. Pictorially it is easy to see that this tunnelling event correspond to a monopole event in the space-time *i.e.* to a creation of a full skyrmion.

Taking into account the Berry phase effect, as we said in the previous section, Q can change only by ± 4 . Then the only allowed terms in the action are proportional to $(\psi_1\psi_2^\dagger)^4$ or $(\psi_2\psi_1^\dagger)^4$.

Consider now the CP^1 representation. We have that

$$n^+ = n_x + in_y = z_1^* z_2 \quad (2.3.3)$$

$$n_z = |z_1|^2 - |z_2|^2 \quad (2.3.4)$$

In this case a 2π vortex in n^+ corresponds to

- 2π vortex in z_1 and no vortex in z_2

or

- 2π antivortex in z_2 and no vortex in z_1

In the first case we have that at the core z_1 goes to zero and then $n_z = -|z_2|^2$ is negative. Thus it corresponds to a ψ_2 meron. Similarly it is easy to see that the

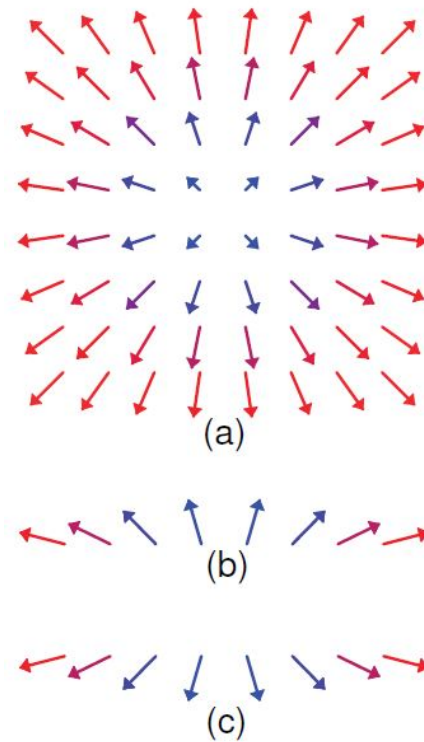


Figure 2.4: Merons vortices in easy plane case. In (a) the vector (n_x, n_y) is represented, that is the same for both ψ_1 and ψ_2 vortices. Instead in (b) and (c) the component (n_x, n_z) respectively of ψ_1 and ψ_2 are shown. From [29]

second case corresponds to a ψ_1 meron.

It is interesting to look at the dual form of this model. First notice that in the easy plane limit we have

$$|z_{i1}|^2 - |z_{i2}|^2 \simeq 0 \quad (2.3.5)$$

$$|z_{i1}|^2 + |z_{i2}|^2 = 1 \quad (2.3.6)$$

These relations allow us to write the $z_{i\alpha}$ in this way:

$$z_{i\alpha} \sim \frac{1}{\sqrt{2}} e^{i\phi_{i\alpha}} \quad (2.3.7)$$

with $\phi_{i\alpha} \in [0, 2\pi)$ and $\alpha = 1, 2$. The index "i" labels the position on the cubic lattice in $D = 2 + 1$ dimensions. A model related to (2.1.8) in terms of the spinon field $z_{i\alpha}$ is the Sachedev-Jalabert (SJ) one [30]:

$$\mathcal{S}_{SJ} = \mathcal{S}_z + \mathcal{S}_a + \mathcal{S}_B \quad (2.3.8)$$

$$\mathcal{S}_z = -t \sum_i z_{i\alpha}^* e^{ia_\mu} z_{i+\hat{\mu},\alpha} + c.c. \quad (2.3.9)$$

$$\mathcal{S}_a = \frac{K}{2} \sum_{i,n} (\epsilon_{\mu\nu\lambda} \Delta_\nu a_\lambda - 2\pi q_\mu)^2 \quad (2.3.10)$$

$$\mathcal{S}_B = i \frac{\pi}{2} \sum_n \zeta_n \Delta_\mu q_\mu \quad (2.3.11)$$

Here Δ_μ is the discrete derivative, a_μ is the compact $U(1)$ gauge field and q_μ is an integer gauge flux defined on the link of the dual lattice. ζ_n can be 0, 1, 2, 3 with "n" that labels the site of the dual lattice. The continuum limit of this action neglecting both Berry phase and compactness, *i.e.* setting $q_\mu = 0$, leads to (2.2.4).

Now putting the relation for $z_{i\alpha}$ of Eq. (2.3.7), inside Eq. (2.3.9), we obtain

$$\mathcal{S}_z = -t \sum_{l,\alpha} \cos(\Delta\phi_\alpha - \mathbf{a}) \quad (2.3.12)$$

where Δ and \mathbf{a} are vectors with components respectively Δ_μ and a_μ , and "l" label the links of the cubic lattice.

From the usual boson-vortex duality [30, 28, 11] the dual action in terms of the merons field can be written as

$$\begin{aligned} \mathcal{L}_{dual} = & \sum_{a=1,2} |(\partial_\mu - iA_\mu)\psi_a|^2 + s_d |\psi|^2 + u_d (|\psi|^2)^2 + \omega_d |\psi_1|^2 |\psi_2|^2 + \\ & + k_d (\epsilon_{\mu\nu k} \partial_\nu A_k)^2 - \lambda [(\psi_1^* \psi_2)^4 + (\psi_2^* \psi_1)^4] \end{aligned} \quad (2.3.13)$$

where $|\psi|^2 = |\psi_1|^2 + |\psi_2|^2$. The fields $\psi_{1,2}$ destroy meron vortices. As usual for the dual theories [30] these fields are coupled with a *non-compact* gauge field A_μ . Physically this is related to the conservation of $j_\mu = \epsilon_{\mu\nu\lambda}\partial_\nu A_\lambda/\pi$, which is the current of S^z . Thus the spin density and the spin current are related with the dual magnetic and electric fields. The Z_2 symmetry $n^z \rightarrow -n^z$ corresponds to the exchange of the two vortices $\psi_1 \rightarrow \psi_2$.

Clearly the ω_d term is due to the easy-plane anisotropy of the model, while λ term can be interpreted as the vortex fugacity. Notice that if we neglect the monopole events, we know that there is another conserved quantity: the total skyrmion number Q or equivalently the difference of the total number of either kind of vortices. Thus we expect an other conservation law appearing in this dual theory. Indeed if we ignore the last term in the lagrangian (2.3.13), a $U(1)$ symmetry appears

$$\psi_1 \rightarrow \psi_1 e^{iq} \tag{2.3.14}$$

$$\psi_2 \rightarrow \psi_2 e^{-iq} \tag{2.3.15}$$

where q is a constant.

However if we restore the monopole term in Eq. (2.3.13), this symmetry is broken but there is still a discrete Z_4 symmetry. This is perfectly consistent with the fact that skyrmion number is still conserved *modulo 4* ($\Delta Q = \pm 4$), as shown by Haldane [9, 30].

It's important to note that XY ordered phase, in the dual theory corresponds to a dual paramagnetic phase where $\langle \psi_{1,2} \rangle = 0$ and $\psi_{1,2}$ fields are gapped [29, 30]. Instead the spin paramagnetic phase corresponds to a situation in which there is a condensation of the fields $\psi_{1,2}$. In particular if $\langle \psi_1 \rangle = \langle \psi_2 \rangle \neq 0$ there is a global Ising symmetry. It is evident the strong similarity between the dual theory and the theory in term of the spinon fields in Eq. (2.2.4) if we interchange the $z_{1,2} \rightleftharpoons \psi_{1,2}$ and the role of XY order and paramagnetic phase. With $\lambda = 0$, \mathcal{L}_z and \mathcal{L}_{dual} have the same form with the interchange $z_{1,2} \rightleftharpoons \psi_{1,2}$ and $a_\mu \rightleftharpoons A_\mu$. This means the model has a *self-dual* critical point.

It is important to notice that in both direct and dual representation the theory is not described in terms of the "physical" boson (n^+ or the skyrmion creation operator). In fact these are written down in function of the "fractionalized" fields (spinons or meron vortices). The dual representation plays an important role also when we

include again the monopole term. Indeed the non-trivial physics of instantons, is described simply by a local perturbation in the dual theory *i.e.* considering $\lambda \neq 0$.

We now look at the scaling dimension Δ of the $(\psi_1^* \psi_2)^4$, that is the fourth power of the creation operator of the physical boson. This quantity is very useful because it determines the relevance or irrelevance of the monopoles at the self dual $\lambda = 0$ fixed point: if $\Delta > D = 3$ they are irrelevant.

It is possible to just do an estimate of this value by first pointing out that both in the direct and dual representation, the physical bosonic field is actually a composite of fundamental fields of the theory. For this reason we expect the bosonic scaling dimension to be larger than the one the "standard" XY theory. It is well known [7] that for the ordinary XY fixed point, the four-fold symmetry breaking perturbation are irrelevant. Thus it has to be the same for our theory.

We remark the importance of the Berry phase in this framework: it is responsible of the quadrupling of the monopoles and thus of their irrelevance at the quantum critical point. Although λ term is irrelevant at the fixed point, it is instead relevant in the paramagnetic phase, where it plays a central role in the choice of the pattern of translation symmetry breaking. For this reason it is said to be *dangerous irrelevant* term. It also play a determinant role in the confinement of the spinons. This is the reason why it is called a *deconfined* quantum critical point: at this point spinons emerge as natural degrees of freedom whereas in both the ordered phase they are confined within a length scale that diverges at criticality.

2.4 Isotropic case

In order to generalize these results to the isotropic case, *i.e.* $SU(2)$ invariant, it is useful to work in the CP^N representation. If we find that for $N = 1$ and $N \rightarrow \infty$ there is such a transition, it will be reasonable that it would be also for the $N = 2$ scenario, *i.e.* for the isotropic case.

Let's start with $N = 1$. In this case z is simply a complex number $z = e^{i\phi}$. In this case it is found a transition between a Higgs phase (that corresponds to antiferromagnetic Néel phase for the $N = 2$ case [29]) and a VBS phase [29] and it falls in the 3D XY universality class [29]. Doing the same consideration of the previous section for the duality maps for the $N = 1$ case, we can say that the four-fold anisotropy in the VBS phase is the quadrupled instanton event that is irrelevant

at the $D = 3$ XY fixed point.

For large N , there is the same situation. Let's start with the model all monopoles excluded that is the CP^{N-1} non-compact model. Also here there is an ordering transition [29] associated with the condensation of z . Once again we look at the relevance or irrelevance of the quadrupled monopole events. It is known [22] that the scaling dimension of this operator in the CP^{N-1} model goes as N . Thus for $D = 3$ they are irrelevant.

The fact that a second order transition is possible for $N = 1$ and $N \rightarrow \infty$, is a strong evidence that it works also for the $N = 2$ case. In the isotropic case we do not have the self-duality, that remains a special case of the XY model. However here it is still true that the Berry phase plays a central role: it simplifies the critical theory cancelling the compactness of the gauge field and leading us to neglect monopoles events. Indeed this critical theory corresponds to the classical $O(3)$ model with monopoles suppressed.

2.5 Physical properties

One of the most important result that was shown is the presence of the so called *dangerous irrelevance* of monopole. The $\lambda \equiv \lambda_4$ term is indeed irrelevant at the quantum critical point but it is relevant for the paramagnetic fixed point. This paramagnetic phase of \mathcal{L}_z of Eq. (2.2.4) is actually described as a $U(1)$ spin liquid with a gapless deconfined photon field a_μ . This is known to be unstable to inclusion of monopoles. This means that for λ perturbation the $U(1)$ spin liquid leads to a VBS phase with Z_4 discrete symmetry and confinement of spinons. In Fig. 2.5 the behaviour of the renormalization group is illustrated. The theory given by \mathcal{L}_z of Eq. (2.2.4) describes only the line $\lambda = 0$. Clearly this is the theory for the transition between a Néel and a $U(1)$ spin liquid phase. However our model never has an exactly zero value of λ : monopole events are actually quadruplicated as we have shown in the previous chapter. At the critical point this is irrelevant while it becomes relevant in the paramagnetic phase leading to VBS state.

In order to better understand this behaviour, it is useful to talk about the correlation lengths. The presence of this dangerous irrelevant coupling at the critical point leads to the existence of two different length scales: first there is the spin-spin correlation length ξ which diverges at the transition; then there is an other length

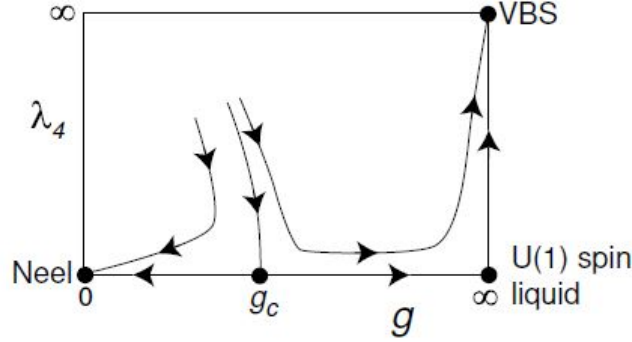


Figure 2.5: Renormalization group flow for $S = 1/2$ square lattice quantum antiferromagnet. From [31]

scale ξ_{VBS} that is associated to the thickness of the domain walls of the VBS order.

On scaling grounds, the two different length are related by [30]:

$$\xi_{VBS} \sim \xi F(\lambda \xi^{3-\Delta}) \quad (2.5.1)$$

where F is a scaling function, Δ is the scaling dimension of the four monopole operator and thus $3 - \Delta$ is the RG eigenvalue of λ . For $r > \xi$ we have the VBS phase that can be seen as an XY order in ψ_{VBS} with weak four-fold anisotropy [30]. Thus variation of the angle θ of the order parameter ($\psi_{VBS} \sim |\psi_{VBS}|e^{i\theta}$) can be considered as pseudo-Goldstone modes [30], whose energy is

$$E(\theta) = \int d^2x \left[\frac{\tilde{K}}{2} |\nabla\theta|^2 - \tilde{\lambda} \cos(4\theta) \right] \quad (2.5.2)$$

where \tilde{K} and $\tilde{\lambda} \propto \lambda$ are parameters renormalized on the scale ξ . From a dimensional analysis we can deduce that [30] $\xi_{VBS} \sim \sqrt{\frac{\tilde{K}}{\tilde{\lambda}}}$ and thus $\xi_{VBS} \sim \lambda^{-1/2}$. Substituting $F(x) \sim x^{-1/2}$ in Eq. (2.5.1), we obtain

$$\xi_{VBS} \sim \xi^{(\Delta-1)/2} \quad (2.5.3)$$

As we have already said, the scaling dimension of the fourth power of the monopole creation operator Δ is greater than 3. This implies that $(\Delta - 1)/2 > 1$ and thus the ξ_{VBS} diverges faster than ξ at criticality.

Considering a point near the transition from the paramagnetic side. At the ξ scale there is a crossover between the critical fixed point of \mathcal{L}_z to the unstable $U(1)$

spin liquid fixed point. The confinement of spinons and the appearance of VBS order occurs at length $\xi_{VBS} > \xi$. We remark that instead in the "traditional" $O(n)$ model described by Eq. (1.1.1) the renormalization flow goes from a fixed critical point to a *stable* paramagnetic critical point.

A consequence of the deconfined critical points is the appearance of the conserved charge *i.e.* the skyrmions number

$$Q = 1/(2\pi) \int d^2x (\partial_x a_y - \partial_y a_x) \sim \int d^2x f \quad (2.5.4)$$

where f is the flux density. The conservation of this quantity fixes its scaling dimension, $\langle f(R)f(0) \rangle \sim \frac{1}{R^4}$. Going away from the criticality this remains true at scale of $R \ll \xi$. Then there is an intermediate scale $\xi \ll R \ll \xi_{VBS}$ where the flux correlation decays as $\frac{1}{R^3}$ [29]. This is characteristic of theory with presence of free photons. For scale $R \gg \xi_{VBS}$ there is VBS order.

As we have already said this new phase transition does not fall in the standard $O(3)$ universality class. This leads to the possibility to have large value of the anomalous dimension η of Eq. (1.1.6). In fact the spinon z_α propagator is $1/p^2$, where p is the 3 space-time momentum. However the Néel order parameter is a composite of spinons ($\hat{n} = z^\dagger \vec{\sigma} z$) and thus the dynamical susceptibility involves the convolution of two of such propagators with momenta p_1 and $p + p_1$:

$$\chi(p) \sim \int \frac{d^3 p_1}{p_1^2 (p + p_1)^2} \sim \frac{1}{|p|} \quad (2.5.5)$$

Comparing this relation with Eq. (1.1.6), it is easy to see that we expect a value of η near 1. Precise calculations [30] show that $\eta \simeq 0.6$.

Chapter 3

Monte Carlo Simulations

In the previous chapter we have seen that the theory of the "traditional" LGW quantum transition of a $O(3)$ rotor model between a Néel and a paramagnetic phase in two dimensions, is the same of the classical 3D $O(3)$ Heisenberg model. Moreover a second order Néel-VBS transition, is described by a classical 3D $O(3)$ model with hedgehog suppression.

Close to a critical point the mean value of observables, such as the order parameter, has anomalous behaviours that are usually expressed in terms of power laws. Their exponents are called *critical exponents* [23]. The critical exponents are a very powerful tool because they assume the same value for all the system that belong to the same *universality class* [23].

In this work we will consider three particular critical exponents β , ν and the anomalous dimension η , defined as

$$\begin{aligned} M &\sim (T_c - T) \\ \xi &\sim |T - T_c|^{-\nu} \\ G(r) &\sim \frac{1}{r^{-(d-2+\eta)}} \quad (T = T_c) \end{aligned} \tag{3.0.1}$$

where M is the order parameter *i.e.* the magnetization, ξ is the spin-spin correlation length and $G(r)$ is the *correlation function* for two spin separated by a distance r .

In order to study the universality classes of these models, we have simulated them with Monte Carlo methods (see Appendix C).

3.1 Classical Heisenberg model

Let's start by considering the Heisenberg Hamiltonian with ferromagnetic interactions:

$$\mathcal{H} = -J \sum_{\langle ij \rangle} \vec{S}_i \cdot \vec{S}_j \quad (3.1.1)$$

Here $J = 1/T$ is the positive coupling constant, T is the temperature and the sum is between the nearest neighbour sites.

In order to realize some numerical simulations we consider a finite cubic system of size L with *periodic boundary conditions* in which each spin is represented as a three dimensional unitary vector. For this reason is convenient to *control* each spin with two parameters: the two polar angles θ and ϕ . A configuration of the system is uniquely defined by assigning to each spin a specific value for those angles with $\phi \in [0, 2\pi[$ and $\theta \in [0, \pi[$.

To bring the system to equilibrium and extract the value of some useful observable (like magnetization) we use the *single-flip Metropolis algorithm*, described in the Appendix C. A random configuration for a single spin is given by randomly choosing the two parameters θ and ϕ from

- $\phi = 2\pi u$
- $\cos^{-1}(2\nu - 1)$

where u and ν are random variables distributed uniformly in the interval $(0, 1)$. In this way we have a unit vector with uniform probability distribution on the S_2 sphere [33].

Once we have chosen a starting configuration, the *single-flip Metropolis algorithm* allows us to evolve our system by accepting or rejecting new configurations (obtained by simply changing the direction of a spin at random) with a probability

$$e^{-\frac{\Delta E}{T}} \quad (3.1.2)$$

where ΔE is the difference between the energy of the new and the old configurations (see Appendix C).

The repetition of this procedure $L \times L \times L$ times forms a *Monte Carlo sweep* (MCS). For each of MCS we calculate the value of some observable that we are

3.1. Classical Heisenberg model

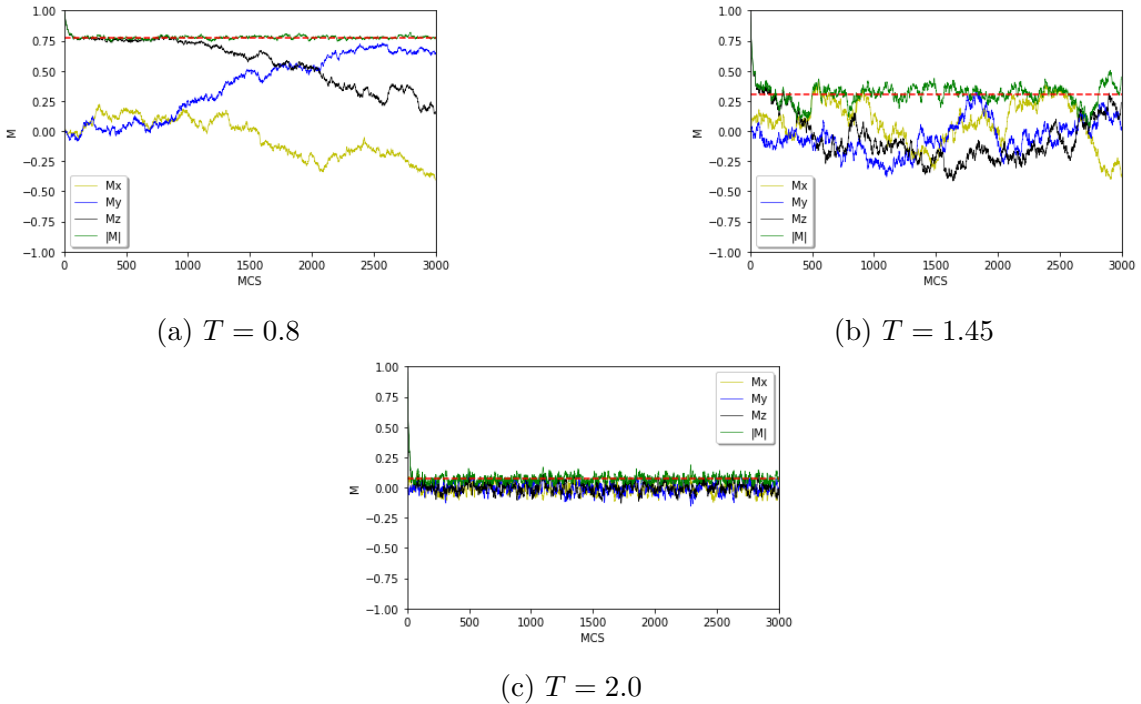


Figure 3.1: The evolution of the three components M_x , M_y , M_z and the modulus M of the magnetization in 3000 MCSs at (a) $T = 0.8$, (b) $T = 1.45$ and (c) $T = 2.0$. The dashed red line represents the mean value $\langle M \rangle$.

looking for and then we take the mean value over all sweeps. Here, we are interested in the magnetization per spin M which is simply the sum of all the single spin magnetizations divided by L^3 :

$$M = \frac{1}{L^3} \left| \sum_i \vec{S}_i \right| \quad (3.1.3)$$

The typical behaviour of M as a function of the number of sweeps for three different temperature is shown in Fig. 3.1. As we can see the starting configurations are chosen to have all vectors directed along the z axis, giving a magnetization $M = 1$, but this choice is not relevant for our purpose because of the $O(3)$ symmetry of the system. In fact it is easy to see that the three components exchange with each other. At $T = 0.8$ it is evident that there is a non zero magnetization and thus we are clearly in the ordered phase; on the other hand at $T = 2.0$ the value of M seems to be near the zero suggesting that the system is in the paramagnetic phase.

3.1. Classical Heisenberg model

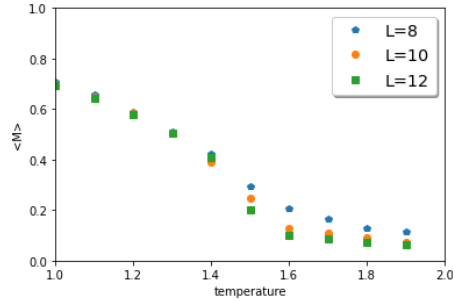


Figure 3.2: Mean value of magnetization as a function of temperature for $L=8,10,12$. We can see that in the disordered phase magnetization goes to values near the zero as fast as L grows.

The mean value of magnetization is simply the arithmetic mean on the MCSs

$$\langle M \rangle = \frac{1}{N_{MCS}} \sum_{t=1}^{N_{MCS}} M_t \quad (3.1.4)$$

where N_{MCS} is the total number of MCS. For each value of $\langle M \rangle$, 3000 MCSs have been performed, of which 1000 was used to reach thermodynamic equilibrium. This means that the mean value of magnetization is calculated by using only the last 2000 of MCSs.

It's interesting to study the behaviour of the magnetization as a function of the temperature as we see in Fig. 3.2. It's easy to notice that the magnetization has the form of an order parameter. In the paramagnetic phase the magnetization goes to values near to zero as L becomes bigger.

Another interesting quantity to study is the specific heat [3]:

$$C_V = \frac{\langle E^2 \rangle - \langle E \rangle^2}{T^2} \quad (3.1.5)$$

where E is the energy per site. As we can notice in Fig. 3.3 the specific heat peaks around $T = 1.4$.

One possible methods to find out the critical temperature is to use the *fourth-order Binder parameter* U_L defined as [3, 24, 10]:

$$U_L(T) = 1 - \frac{1}{3} \frac{\langle M^4 \rangle}{\langle M^2 \rangle^2} \quad (3.1.6)$$

For $O(n)$ model it is known [10] that in the high temperature limit $U_L \rightarrow 2(n-1)/3n$. Thus $n = 3$ it tends to $4/9$. On the other hand for low temperatures $\frac{\langle M^4 \rangle}{\langle M^2 \rangle^2} \simeq 1$ and

3.1. Classical Heisenberg model

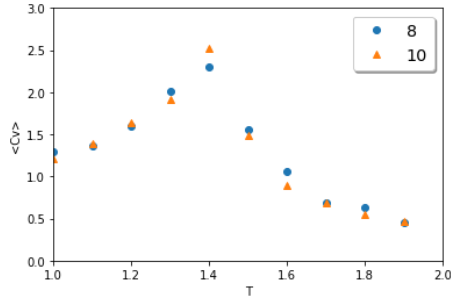


Figure 3.3: Specific heat for system with $L = 8$ and $L = 10$. The peak is for $T \simeq 1.4$

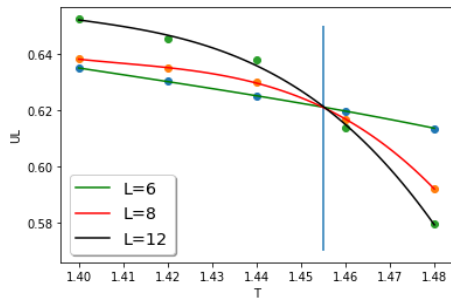


Figure 3.4: Binder parameter for $L = 6, 8, 12$. It's clear that the intersection point is around $T \simeq 1.455$.

Binder parameter goes to $2/3$ [10]. Considering the behaviour of U_L as a function of the temperature, finite-size scaling implies [3] that the curves $U_L(T)$ for different values of size L should intersect at a point. This point corresponds to the critical temperature T_c .

For this reason we compute the value of U_L in the range between $T = 1.40$ and $T = 1.5$ for $L = 6, 8, 12$. In Fig. 3.4 it is reported the behaviour of U_L . The critical temperature is evaluated by looking at the intersection point of these three curves and its value is $T_c = 1.455$. In order to take a specific value for T_c we have considered the ratio $U_{L'}/U_L$ ($L' = 12$ and $L = 8$) in the range $1.44 < T < 1.46$ and we have seen where it intersect the straight line $U_{L'}/U_L = 1$. It gives us

$$T_c = 1.45 \pm 0.05 \quad (3.1.7)$$

compatible with the results of [16].

Now we look for the critical exponents ν and β . First of all we derived the value of ν using the relations given by the finite-size scaling analysis. It is known that the

3.1. Classical Heisenberg model

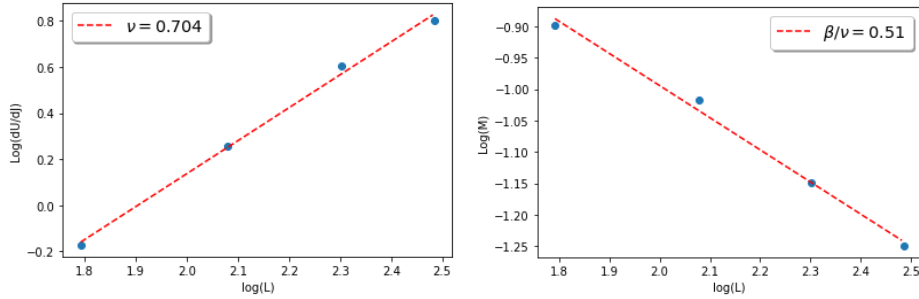


Figure 3.5: At left a log-log plot of the derivative of Binder parameter respect J , $\frac{dU_L}{dJ}(J_c)$. The inverse slope of the straight line is $\nu = 0.704$. At right a log-log plot of the derivative of magnetization $\langle M(J_c) \rangle$. The absolute value of the slope is $\beta/\nu \simeq 0.51$

derivative $\frac{dU_L}{dJ}$ (where $J = 1/T$), goes as $L^{1/\nu}$ near T_c . The derivative can be written in this way [10]:

$$\frac{dU_L}{dJ} = (1 - U_L) \left\{ \langle E \rangle - 2 \frac{\langle Em^2 \rangle}{\langle m^2 \rangle} + \frac{\langle Em^4 \rangle}{\langle m^4 \rangle} \right\} \quad (3.1.8)$$

In Fig. 3.5 we plot the value of $\frac{dU_L}{dJ}(J_c)$ versus L in a log-log scale. Clearly the inverse slope of the line in the left panel of Fig. 3.5 is the value of ν . A best fit yields:

$$\nu = 0.70 \pm 0.05 \quad (3.1.9)$$

The same procedure is performed to obtain the value of β/ν , knowing that

$$\langle M \rangle \sim L^{\beta/\nu} \quad (3.1.10)$$

which is shown in the right panel of Fig. 3.5 in a log-log scale plotting. The value of critical exponent is

$$\beta/\nu = 0.51 \pm 0.04 \quad (3.1.11)$$

The value of the critical exponents is consistent with [16].

To check the correct value of the critical temperature T_c and the critical exponents, we can perform a finite-size scale analysis as reported in Fig. 3.6. Near T_c the magnetization has to satisfy the following law [3]:

$$\langle M(L, T) \rangle = L^{-\beta/\nu} g_1(tL^{1/\nu}) \quad (3.1.12)$$

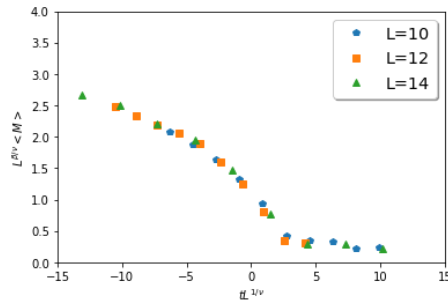


Figure 3.6: Finite-size scaling for $L = 10, 12, 14$ at $T_c = 1.45$. All the three curves overlap.

where $t = (T - T_c)/T_c$ and g_1 is the universal scaling function.

If we use the values obtained above, Eq. (3.1.7), (3.1.9) and (3.1.11), we see from Fig. 3.6 that indeed the three curves overlap for different values of L . This is evidence of the validity of our analysis.

3.2 Topological charge

It is now interesting to look at the role of the topological charge Q in this kind of model. In the continuum limit Q represents the number of times that the spins on a closed surface surrounding the defect cover the surface of a unit sphere and corresponds to (2.1.7).

Since our model is originally described on the lattice we have to discretize this quantity. In order to do this we use the method introduced by Berg and Luscher [2] and generalized by Lau and Dasgupta [16] for cubic lattice: decompose the finite lattice in $L \times L \times L$ cubes with the lattice sites at the vertices; divide each of the six faces of each cube in two equal part by drawing the diagonal. In this way we obtain 12 triangles for each cube. Consider $S_1(i), S_2(i), S_3(i)$ the three spins at the vertices of the i -th triangle ordered going around the circuit $1 \rightarrow 2 \rightarrow 3 \rightarrow 1$ in a counterclockwise rotation, as it is illustrated in Fig. 3.7. It is important to underline that the areas have an orientation given by $S_1(i) \cdot (S_2(i) \wedge S_3(i))$, represented as the red vector in Fig. 3.7. Let be Δ_i the oriented area of the spherical triangle formed by three spins on the surface of a unite sphere. The topological charge in j -th cube

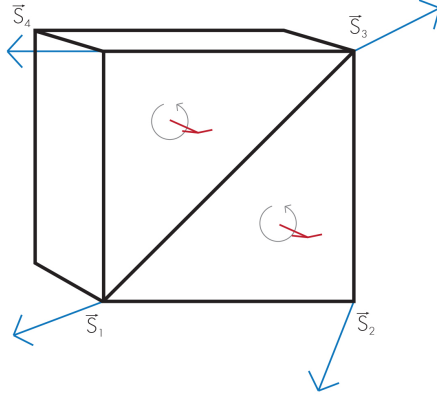


Figure 3.7: A single cube with spins at vertices. The front face of the cube is divided in two equal parts by the diagonal. We calculate the areas of the spherical triangles with vertices spin $\vec{S}_1, \vec{S}_2, \vec{S}_3$ and $\vec{S}_1, \vec{S}_3, \vec{S}_4$. The orientations of the areas are reported in figure with the red vectors. We do the same for all the six faces of the cube.

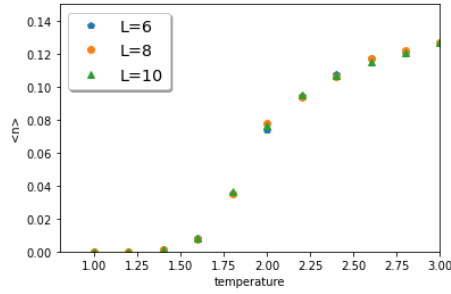


Figure 3.8: Topological defect pair density for different lattice sizes. We can notice that the value of $\langle n \rangle$ is almost the same for all the sizes considered.

will be [16]:

$$Q_j = \sum_{i=1}^{12} \Delta_i \quad (3.2.1)$$

Because of the fact that we are working with period boundary conditions, the total $Q_{tot} = \sum_j Q_j$ of the whole lattice is zero (we remark that we usually start with a configuration with all spin directed along the same direction). In Fig. 3.8 we plot the defect pair density $\langle n \rangle$ as a function of temperature. As we can see, at temperatures smaller than T_c the pair density is near to the zero as one might expect. On the other hand in the paramagnetic phase, *i.e.* at temperature above T_c ,

3.2. Topological charge

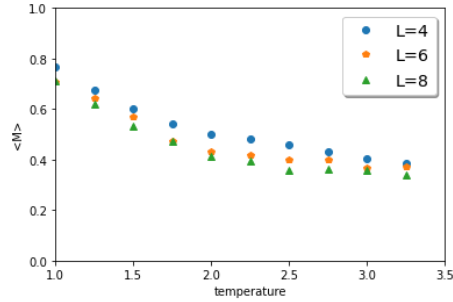


Figure 3.9: Magnetization as a function of temperature with no defects allowed. As we can see the magnetization tends to stay on non-zero values.

$\langle n \rangle$ starts to rapidly increase [16].

We can ask ourselves what would happen if we neglect this topological defects in the paramagnetic phase and what is their role in the 3D Heisenberg transition.

Formally we have to consider a new Hamiltonian of the form [16],

$$\mathcal{H} = -J \sum_{\langle ij \rangle} \mathbf{S}_i \cdot \mathbf{S}_j + \lambda \sum_{cubes} |Q| \quad (3.2.2)$$

where now the new parameter $\lambda > 0$ has the role of a sort of chemical potential for defects

Clearly the case of $\lambda \rightarrow \infty$ corresponds to a situation in which the defects are totally forbidden. To numerically simulate the limit with Monte Carlo method, we initialize our system in a fully polarized configuration and then check, after the update of a spin, if a defect pair has appeared in two of the eight cubes that contain the spin. If it did, we reject the new configuration and start over, if not we accept it with a probability $e^{-\frac{\Delta E}{T}}$.

Fig. 3.9 shows how the magnetization per spin as a function of the temperature if the defects are not allowed *i.e.* with $\lambda \rightarrow \infty$. It is important to notice that the magnetization is different from zero also at temperature bigger than 1.45 and it seems that there is no transition at all.

To support this thesis, we just compute the magnetization at $T \rightarrow \infty$ by simply considering $J = 1/T = 0$. In this case the probability to accept a new configuration in Metropolis algorithm becomes simply 1 or 0. For $L = 8$ the value of $\langle M \rangle$ at infinite temperature is $\langle M \rangle \simeq 0.22$, as it is shown in Fig. 3.10. However a precise demonstration of the absence of this transition is reported in [16].

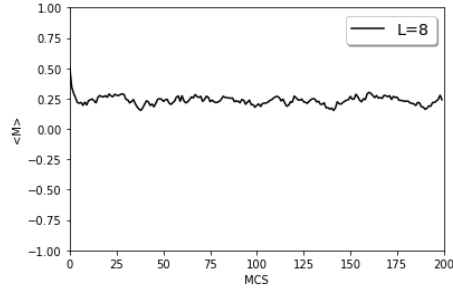


Figure 3.10: Magnetization at infinite temperature with no defect allows. For $L = 8$ the magnetization is about 0.22.

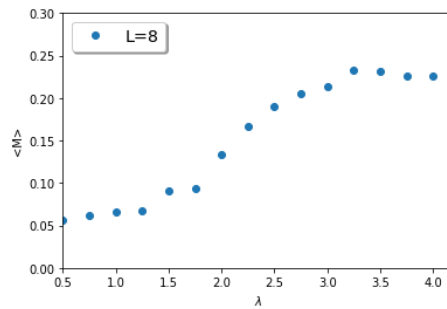


Figure 3.11: Magnetization at infinite temperature as a function of λ . For small values of λ , magnetization has a value near to zero, while it reaches the value of about 0.22 as λ increases.

It is also interesting to understand how the magnetization behaves at infinite temperature varying the parameter λ . From Fig. 3.11, $\langle M \rangle$ is almost zero for small values of λ and then starts to increase. For $\lambda > 3$, $\langle M \rangle$ reaches the value of about 0.22, in agreement with [16].

3.3 Hedgehog Suppression

3.3.1 Close pairs

In the previous section we have found that, neglecting all the configurations which contain hedgehog, there is no transition at all. Magnetization per spin remains different from zero also for infinite temperature. Now we look for configuration in which only single hedgehogs are neglected, allowing pairs $(+1, -1)$ of defects to exist,

+	-	0	0	0
0	+	-	0	0
0	0	+	0	0
0	0	-	0	0
0	0	0	0	0

Figure 3.12: Example of an acceptable configuration of hedgehogs. For simplicity it is represented just a section of the cubic lattice. Here the label + (-) stay for a +1 (-1) hedgehog. It's easy to see that each +1 has a -1 close to it. Clearly one has to check for the same conditions also for hedgehogs above and below the section.

as proposed in [13]. This model is called $O(3)$ $NL\sigma$ model with *hedgehog suppression* [13, 19].

We will see that in this case there is a transition and we conclude that single hedgehogs are not fundamental in this contest. The universal class will be different from the one of the classical $O(3)$ Heisenberg model. In particular a higher value for the anomalous dimension is found, with $\eta \simeq 0.6$.

As in the previous simulations, we have considered a three dimensional cubic lattice of size $L = 6, 8, 10$. We use the same methods described above [2, 16] to discretize topological defects *i.e.* hedgehogs. In this case we allow near pairs (+1, -1) of hedgehog to exist and we mark each pair that appears with a specific label, which allows to keep track of it as we perform the Monte Carlo update. In this way we are able to reject any configuration in which two hedgehogs (+1, -1) belonging to two different pairs, annihilate forming in this way two single hedgehogs. A pair can have many other pairs near it as long as each +1 has "its own" -1 close to it. An example of an acceptable configuration is shown in Fig. 3.12.

In Fig. 3.13 the magnetization per spin is shown for systems with size $L = 6, 8, 10$ as a function of $J = 1/T$. Also in this case, for each value of $\langle M \rangle$, 3000 MCSs have been generated, of which only the last 2000 were used to calculate the mean

3.3. Hedgehog Suppression

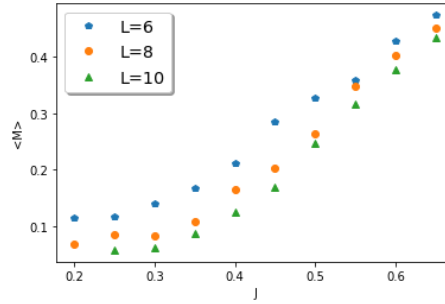


Figure 3.13: Magnetization as a function of $J = 1/T$. We can see that for $J < 0.40$ the magnetization is near to zero as long as L become bigger.

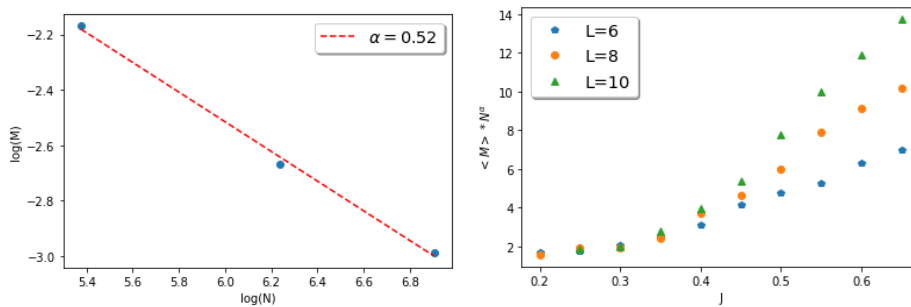


Figure 3.14: Left: the log-log plot between the magnetization and $N = L^3$ at $J = 0.2$. The slope give us the exponent $\alpha \simeq 0.52$. Right: plot of the magnetization multiplied by N^α . It's easy to see that the curves start to overlap for $J < 0.40$

value of observables. We point out that we could not use large values of lattice size because the algorithm used to reject single hedgehog configurations takes much more time then the first used in the previous section. We can notice that for J smaller than 0.3 the value of magnetization goes to values around zero as long as the size increases suggesting that we are in a paramagnetic phase.

In the disordered phase it is expected [19] that $\langle M \rangle \sim c \frac{1}{N^\alpha}$, where $N = L^3$ and c is a constant. Then:

$$\log(M) = -\alpha \log(N) + \log(c) \quad (3.3.1)$$

It is easy to see in Fig. 3.14 by a log-log plotting done at $J = 0.20$, that $\alpha \sim 1/2$. In Fig. 3.14, the magnetization multiplied by $N^{1/2}$ is shown as a function of J . We can easily notice that the values of $\langle M \rangle \cdot N^{1/2}$ for different sizes overlap for $J < 0.40$, and it is reasonable to consider this a paramagnetic phase. On the other

3.3. Hedgehog Suppression

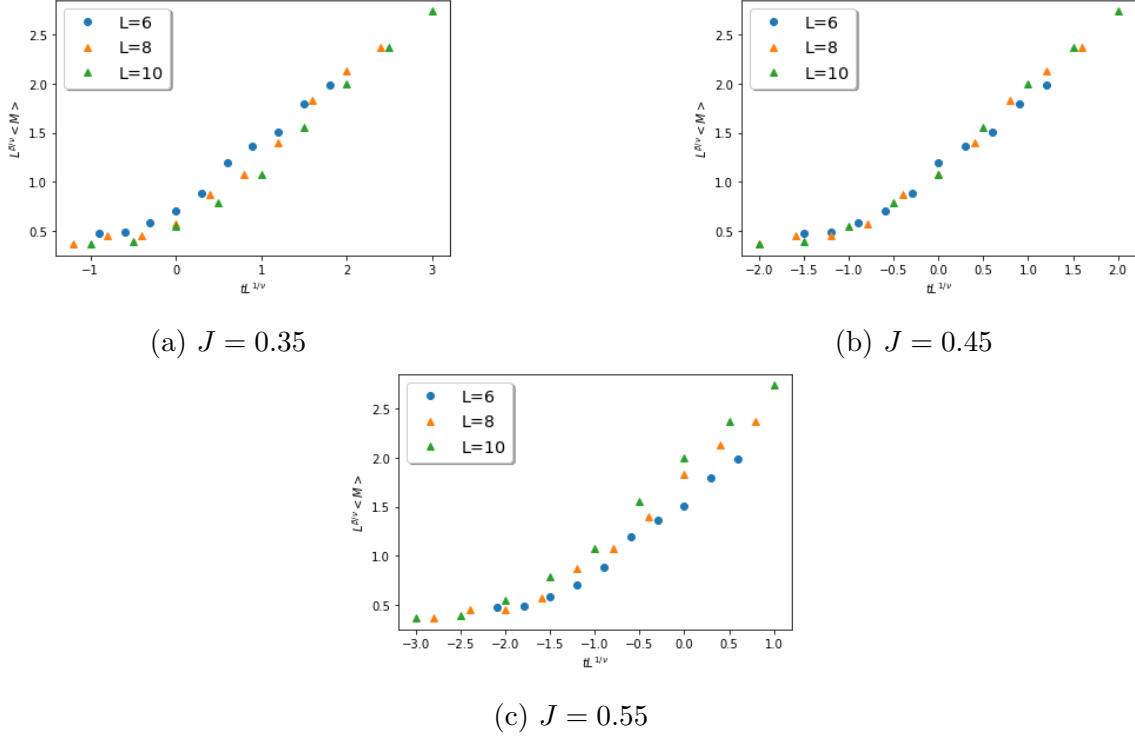


Figure 3.15: Three plots of finite-size scaling at (a) $J = 0.35$, (b) $J = 0.45$, (c) $J = 0.55$ with $\beta = 0.80$ and $\nu = 1.0$. It's clear that the curves overlap for J_c near 0.45.

hand for $J > 0.5$ the magnetization increases as the size becomes bigger. Thus we expect that the critical temperature is in the range $0.40 \leq J_c \leq 0.50$.

In this contest the binder parameter U_L defined above, gives not very precise results: its value oscillates in a uncontrolled way and this does not allow us to estimate the critical temperate T_c (or equivalent J_c) using that method.

Thus as reported in Fig. 3.15 we perform a finite size scaling, for three different value of J_c , using $\nu = 1.0$ and $\beta = 0.80$. These are the values of critical exponents of the classical $O(3)$ Heisenberg model with hedgehog suppression derived by Montrunich and Vishwanath [19].

It is clear that the reasonable value for J_c is $J_c \simeq 0.45$ *i.e.* $T_c \simeq 2.22$. Computing the magnetization at this value of J and remarking that

$$\langle M \rangle \sim L^{\beta/\nu} \quad (3.3.2)$$

3.3. Hedgehog Suppression

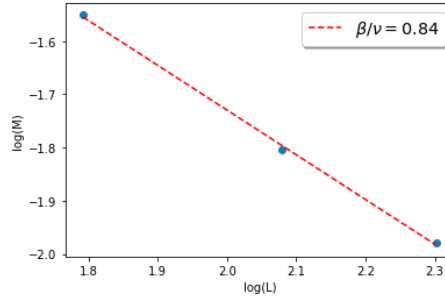


Figure 3.16: Log-log plot of the magnetization vs the size L . The absolute value of the slope gives us $\beta/\nu = 0.84$

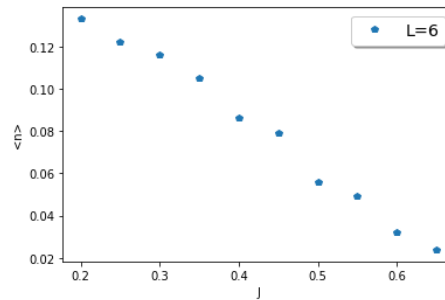


Figure 3.17: Pair defect density $\langle n \rangle$ as a function of J . It tends to go to zero in the ordered phase.

we can simply use the log-log plot as shown in Fig. 3.16 to estimate β/ν . The value is

$$\beta/\nu = 0.84 \pm 0.05 \quad (3.3.3)$$

compatible with [19].

We also report in Fig. 3.17 the behaviour of the pair defect density, defined as in the previous section. It is easy to notice that $\langle n \rangle$ decreases as J becomes bigger. Moreover it tends to zero when $J > 0.5$. It is consistent with the fact that we do not expect the defect to be in the ordered phase.

This transition belongs to a universality class different from that of the standard $O(3)$ Heisenberg model. In particular these values of the critical exponents leads to a big anomalous dimension η . In fact from the scaling laws that relate all the critical exponents [23], it is easy to find that $\eta = (2 - D) + 2\frac{\beta}{\nu} \simeq 0.6$. This value is compatible with that expected for the Néel-VBS transition described in the previous

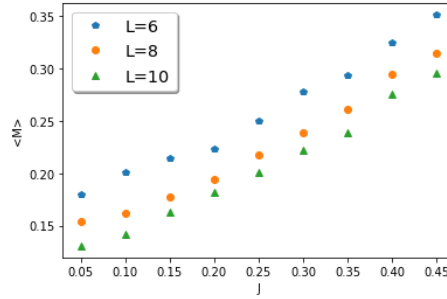


Figure 3.18: Magnetization as a function of J . It tends to go to zero for small J .

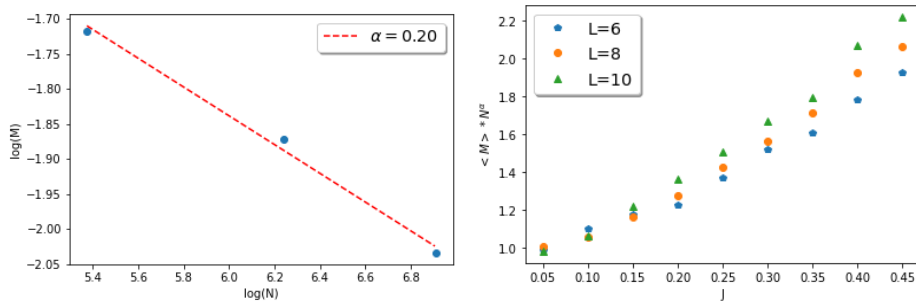


Figure 3.19: Left: the log-log plot of the magnetization and $N = L^3$ at $J = 0.2$. The slope gives us the exponent $\alpha \simeq 0.20$. Right: plot of the magnetization multiplied by N^α . The curves tend to overlap for $J < 0.15$.

chapter.

3.3.2 Isolated pairs

Another way to neglect single hedgehog configurations, is to consider *isolated pairs* $(+1, -1)$ as proposed by Montrunich and Vishwanath [19]: this differs from the previous algorithm because a $+1$ hedgehog can have only one -1 near to it. The procedure is the same as before: we have found the magnetization in function of J , as shown in Fig. 3.18. 3000 MCSs have been performed for each value of $\langle J \rangle$. Also in this case only the last 2000 steps are used to calculate $\langle M \rangle$. Also in this case we use the relation (3.3.1) to find the exponent α such that $\langle M \rangle \sim c \frac{1}{N^\alpha}$. In the left panel of Fig. 3.19 it is shown that $\alpha = 0.2$. In the right panel of 3.19 instead we plot the magnetization per spin $\langle M \rangle$ multiplied by N^α , and it is clear that the magnetization for different sizes tends to overlaps. Considering the critical

3.3. Hedgehog Suppression

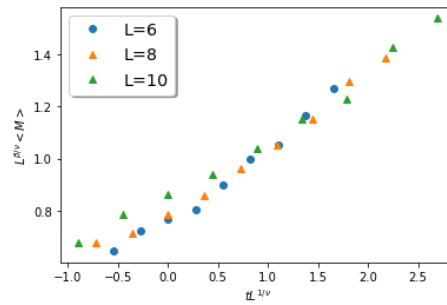


Figure 3.20: Finite-size scaling at $J_c = 0.15$. The curves tend to overlap.

exponents of [19], $\beta = 0.8$ and $\nu = 1.0$, a finite-size scaling is done for $J_c = 0.15$, and it is reported in Fig. 3.20.

We can conclude that, also in this case, there is phase transition, of the same universality class. Clearly the critical value J_c is not equal to the previous one simply because the allowed configurations are different: here we just look for isolated pairs, and then a large number of configurations are rejected. Qualitatively we can justify this two different values of J_c by thinking that at the same J in this case we have a smaller pair density and thus a bigger magnetization. This means that we need a smaller value of J to reach magnetization near to zero *i.e.* paramagnetic phase.

Chapter 4

Conclusions

The main goal of this work was to study the second order quantum transition between the Néel and the VBS phase. As already emphasized this is found to be naturally described in terms of a new degree of freedom, the gauge field a_μ . This field mediates the interaction between the fractional particles (*spinons*) z_α that carry fraction of quantum number of a_μ .

In order to understand this theory, it is important to highlight the role played by the Berry phases of (2.1.6) in this framework. This is not vanishing when the number of skyrmions Q changes. Precise calculations lead to a quadrupling of monopoles events *i.e.* the Q is allowed to change only by 4. This phenomenon increases the scaling dimension of the monopoles. In fact the forth-power of the monopoles creation operator $(\psi_1^* \psi_2)^4$, with scaling dimension Δ , is the only allowed. Δ is found to be greater than $D = 3$, and thus monopoles become *irrelevant* at criticality.

This kind of critical point is characterized by another quantity: a conserved charge that emerges only at the transition. The absence of monopole events at criticality means that in this context the conserved quantity is the skyrmions number Q . Because it corresponds also to the flux of the gauge field a_μ , it is reasonable to neglect the compactness of this field. The theory describes the transition between a Néel and a $U(1)$ spin liquid state, that is *unstable* under perturbations of λ , the monopole fugacity. Actually monopoles are said to be *dangerous irrelevant*, because, while they are irrelevant at QCP, they are relevant in the paramagnetic phase and their proliferation leads to the VBS state.

In this framework we have two kinds of correlation lengths: ξ that is the "stan-

ard" spin-spin correlation length and ξ_{VBS} that represents the thickness of the domain walls of the VBS order. Both these two lengths diverge at criticality and in particular ξ_{VBS} diverges faster than ξ . In the VBS phase spinons are confined at lengths of the order of ξ_{VBS} , while they naturally appear at QCP.

In order to find critical exponents of this theory we numerically simulated with Monte Carlo methods, the 3D classical $O(3)$ Heisenberg model with monopole suppression. We started from studying a "standard" Heisenberg model and its ferromagnetic-paramagnetic transition. Then we have seen that neglecting all the configurations that contain monopoles there is no transition. On the other hand allowing pairs of monopoles to exist, neglecting in this way only single monopoles, a transition appears. We have found out the critical exponents: in particular there is a big anomalous dimension $\eta \simeq 0.6$, very different from that of the "standard" Heisenberg transition.

A purpose for future works may be to study the model in which the condition of having configurations with only pairs of monopoles enters in the Heisenberg Hamiltonian with single monopoles suppressed by means of a chemical potential λ . In this framework the model studied in this work is simply the $\lambda = 0$ version of the new one. In the limit $\lambda \rightarrow \infty$, pairs of monopoles are completely neglected, as single monopoles. In this case we have seen that there is no transition. Thus, it would be interesting to study what happens for finite values of the chemical potential and check when the phase transition disappears.

Appendix A

Non linear sigma model

Here we will discuss quantum antiferromagnet systems focussing on the two dimensional ones. In order to do this, we start with the study the spin coherent states and the path integral construction for this kind of models.

A.1 Spin coherent states

We begin discussing a very simple system: a spin- S degree of freedom coupled to an external field through a Zeeman term. In this case it is known that the $(2S + 1)$ -fold degeneracy is lifted by the interaction and we get $2S + 1$ non degenerate levels [8]. For the construction of the path-integral we are going to use the method of coherent states, reviewed by A. Perelomov in the 1986 [25].

Let us start from the description of the Hilbert space. We have $2S + 1$ states that transform like the spin- S representation of $SU(2)$. We can denote the highest-weight state in the representation as

$$|0\rangle = |S, S\rangle \tag{A.1.1}$$

This is an eigenstate of S_3 and \vec{S}^2 [8]:

$$S_3 |0\rangle = S |0\rangle \tag{A.1.2}$$

$$\vec{S}^2 |0\rangle = S(S + 1) |0\rangle \tag{A.1.3}$$

We can define our coherent state by a rotation of the $|0\rangle$ state [8]:

$$|\vec{n}\rangle = e^{i\theta(\vec{n}_0 \times \vec{n}) \cdot \vec{S}} |S, S\rangle \tag{A.1.4}$$

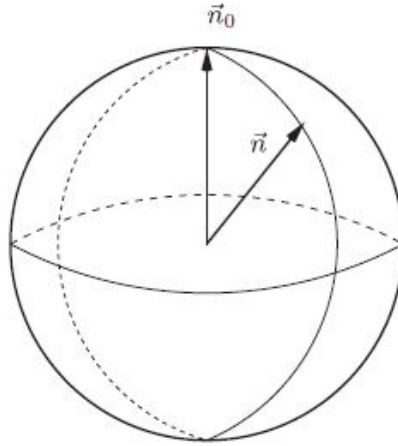


Figure A.1: Unit S_2 sphere. From [8].

This coherent state is labelled by a unit vector \vec{n} that is related with θ and \vec{n}_0 in the following way:

$$\vec{n} \cdot \vec{n}_0 = \cos\theta \quad (\text{A.1.5})$$

where \vec{n}_0 is along the quantization axis. The vector \vec{S} has as components the three generators of $SU(2)$. Consider now the complete basis $|S, M\rangle$, where M labels the eigenvalue of S_3 :

$$S_3 |S, M\rangle = m |S, M\rangle \quad (\text{A.1.6})$$

$$\vec{S}^2 = S(S+1) |S, M\rangle \quad (\text{A.1.7})$$

We can now write the coherent state $|\vec{n}\rangle$ in terms of that basis [8],

$$|\vec{n}\rangle = \sum_{M=-S}^S D^{(S)}(\vec{n})_{MS} |S, M\rangle \quad (\text{A.1.8})$$

The coefficients $D^{(S)}(\vec{n})_{MS}$ do not form a group but they satisfy the algebra [8]

$$D^{(S)}(\vec{n}_1)_{MS} D^{(S)}(\vec{n}_2)_{MS} = D^{(S)}(\vec{n}_3)_{MS} e^{i\Phi(\vec{n}_1, \vec{n}_2, \vec{n}_3) S_3} \quad (\text{A.1.9})$$

The three unit vector $\vec{n}_1, \vec{n}_2, \vec{n}_3$ lie on the unit sphere S_2 and $\Phi(\vec{n}_1, \vec{n}_2, \vec{n}_3)$ is the area of the spherical triangle with vertices at the three vectors.

This area is not uniquely defined because one can choose the "inner" or the "outer" as we can see from the Fig. A.2. The choice of the area is totally arbitrary

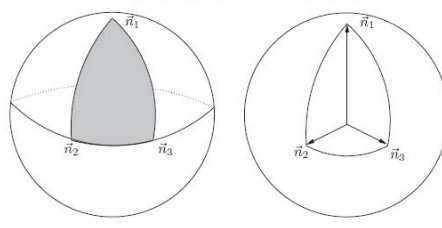


Figure A.2: Inner and outer area of spherical triangle with vertices \vec{n}_1, \vec{n}_2 and \vec{n}_3 . From [8].

because the difference of the two oriented areas is 4π . Then in the path-integral representation this gives a contribute of

$$e^{i4\pi M} = 1 \quad (\text{A.1.10})$$

because M can be just an integer or an half-integer. The area appears in the inner product of two coherent states [8]

$$\langle \vec{n}_1 | \vec{n}_2 \rangle = \langle 0 | D^{(S)\dagger}(\vec{n}_1) D^{(S)}(\vec{n}_2) | 0 \rangle = e^{i\Phi(\vec{n}_1, \vec{n}_2, \vec{n}_0)S} \left(\frac{1 + \vec{n}_1 \cdot \vec{n}_2}{2} \right)^2 \quad (\text{A.1.11})$$

There are other two important relations to point out [8]:

$$\langle \vec{n} | \vec{S} | \vec{n} \rangle = S\vec{n} \quad (\text{A.1.12})$$

and

$$I = \int d\mu(\vec{n}) |\vec{n}\rangle \langle \vec{n}| \quad (\text{A.1.13})$$

where $d\mu$ is the invariant measure

$$d\mu(\vec{n}) = \left(\frac{2s+1}{4\pi} \right) d^3n \delta(\vec{n}^2 - 1) \quad (\text{A.1.14})$$

A.2 Path-integral

In this section we want to construct the path-integral for a one particle system using the notion of *coherent states* defined before.

The partition function is defined as

$$Z = \text{tr} e^{iHT} = \text{tr} e^{-\beta H} \quad (\text{A.2.1})$$

with β the imaginary time. Using the Trotter formula and the identity (A.1.13) we got [8]

$$Z = \lim_{N_t \rightarrow \infty} \left(\prod_{j=1}^{N_t} \int d\mu(\vec{n}_j) \right) \left(\prod_{j=1}^{N_t} \langle \vec{n}(t_j) | e^{-\delta t H} | \vec{n}(t_{j+1}) \rangle \right) \quad (\text{A.2.2})$$

where $N_t \delta t = \beta$. We are considering a closed trajectory of the unit vector \vec{n}_j , with t_j the set of times between $[0, \beta]$. Approximating the exponential with $1 - \delta t H$ and using (A.1.11), we arrive to [8]

$$Z = \lim_{N_t \rightarrow \infty} \int \mathcal{D}\vec{n} e^{-\mathcal{S}_E[\vec{n}]} \quad (\text{A.2.3})$$

where

$$\mathcal{D}\vec{n} = \prod_{j=1}^{N_t} d\mu(\vec{n}_{t_j}) \quad (\text{A.2.4})$$

and

$$-\mathcal{S}_E[\vec{n}] = iS \sum_{j=1}^{N_t} \Phi(\vec{n}_{t_j}, \vec{n}_{t_{j+1}}, \vec{n}_0) + S \sum_{j=1}^{N_t} \ln \left(\frac{1 + \vec{n}_{t_j} \cdot \vec{n}_{t_{j+1}}}{2} \right) - \sum_{j=1}^{N_t} \langle \vec{n}_{t_j} | H | \vec{n}(t_j) \rangle \quad (\text{A.2.5})$$

The first term leads to a sum of trajectories weighted by phases that represent the areas of spherical triangles with vertices $\vec{n}_{t_j}, \vec{n}_{t_{j+1}}$ and \vec{n}_0 . The sum of all this areas is the total area $\mathcal{A}(\Sigma^+)$ of the part of S_2 in which the closed trajectory of \vec{n}_t divides the unit sphere. It is not important which of the two part we choose because

$$\mathcal{A}(\Sigma^+) + \mathcal{A}(\Sigma^-) = 4\pi \quad (\text{A.2.6})$$

and then there is no physical manifestation of this choice.

In the continuum limit ($N_t \rightarrow \infty, \delta t \rightarrow 0$) [1]

$$\mathcal{A}(\Sigma^+) = \int_0^1 d\tau \int_0^\beta dt \vec{n}(t, \tau) \cdot (\partial_t \vec{n}(t, \tau) \times \partial_\tau \vec{n}(t, \tau)) \quad (\text{A.2.7})$$

where

$$\vec{n}(t, 0) = \vec{n}(t), \quad \vec{n}(t, 1) = \vec{n}_0, \quad \vec{n}(0, \tau) = \vec{n}(\beta, \tau) \quad (\text{A.2.8})$$

The total Euclidean action for an single particle system with a Hamiltonian of the form $H(\vec{S}) = \vec{B} \cdot \vec{S}$ becomes [8]

$$\mathcal{S}_E[\vec{n}] = -iS\mathcal{A}[\vec{n}] + S \int_0^\beta dt \vec{B} \cdot \vec{n}(t) \quad (\text{A.2.9})$$

with \vec{B} the external magnetic field.

Generalizing the above procedure we can write the Euclidean action for a many-particle problem with a generic Hamiltonian $\mathcal{H}(t)$ in this way [1, 8]:

$$\mathcal{S}_E[\vec{n}] = -iS\mathcal{A}[\vec{n}] + S \int_0^\beta dt H[\vec{n}(t)] \quad (\text{A.2.10})$$

where

$$H[\vec{n}(t)] = \langle \vec{n}(t) | \mathcal{H}(t) | \vec{n}(t) \rangle \quad (\text{A.2.11})$$

In particular for a antiferromagnetic Heisenberg spin-S system in d dimensions with an Hamiltonian given by

$$\mathcal{H} = J \sum_{\langle \vec{r}, \vec{r}' \rangle} \vec{S}(\vec{r}) \cdot \vec{S}(\vec{r}') \quad (\text{A.2.12})$$

we can write the Euclidean action [1]

$$\mathcal{S}_E[\vec{n}] = -iS \sum_{\vec{r}} \mathcal{A}[\vec{n}(\vec{r})] + \int_0^\beta dt \sum_{\langle \vec{r}, \vec{r}' \rangle} JS^2 \vec{n}(\vec{r}, t) \cdot \vec{n}(\vec{r}', t) \quad (\text{A.2.13})$$

Here we consider a simple cubic lattice of dimension d and the sum is over the nearest neighbor sites. The interaction J gives rise to a Néel ground state for the classical Hamiltonian $H[\vec{n}]$. J is also assumed to be short ranged [1]:

$$\frac{1}{2d} \sum_j |J||\vec{r} - \vec{r}'| < \infty \quad (\text{A.2.14})$$

A.3 Haldane's Mapping

Haldane has showed [8, 1] that the effective action of quantum Heisenberg antiferromagnet in d dimensional cubic lattice can be mapped into a nonlinear sigma model in $d + 1$ dimensions. This can be done using the *Haldane's Mapping*, that is the separation between the short and the long length scale fluctuation[1]:

$$\vec{n}(i) = \eta(i)\vec{m}(i) \sqrt{1 - \left| \frac{\vec{L}(i)}{S} \right|^2} + \frac{\vec{L}(i)}{S} \quad (\text{A.3.1})$$

where $\eta(i) = e^{i\vec{x}(i) \cdot \vec{K}}$ has opposite sign on the two sublattice, with $\vec{x}(i)$ the position on the lattice and $\vec{K} = (\pi, \pi)$. Near the Néel phase, the slowly varying part \vec{m} can be

seen as the *staggered magnetization* unit vector, while the *canting* field \vec{L} represents fluctuations that are always orthogonal to \vec{m} :

$$|\vec{m}(i)| = 1 \quad (\text{A.3.2})$$

$$\vec{L}(i) \cdot \vec{m}(i) = 0 \quad (\text{A.3.3})$$

By performing the continuum limit and expanding the interaction to the quadratic order in $\left|\frac{\vec{L}}{S}\right|^2$, we get [1]

$$\mathcal{S}_E[\vec{m}] = -i\gamma[\vec{m}] + \frac{1}{2} \int_0^\beta d\tau \int_\Lambda d^d x \frac{\rho_s}{c} \left(\frac{1}{c} |\partial_\tau \vec{m}|^2 + c \sum_{l=1}^d |\partial_l \vec{m}|^2 \right) \quad (\text{A.3.4})$$

where ρ_s is the *spin stiffness constant* and c_s is the *spin wave velocity*. The first term is the *topological Berry phase* in terms of the *Néel field* \vec{m} [1],

$$\gamma[\vec{m}] = S \sum_i \eta(i) \mathcal{A}[\vec{m}(i)] \quad (\text{A.3.5})$$

It is easy to see that the second term is an action of a non linear sigma-model in $d + 1$ dimensions. In fact we just make the transformation

$$(x_1, \dots, x_d, c\tau) \rightarrow (x_1, \dots, x_{d+1}) \quad (\text{A.3.6})$$

and we have [1, 8]

$$\mathcal{S}_E[\vec{m}] = -i\gamma[\vec{m}] + \int d^{d+1} \mathcal{L}_{NLSM}^{d+1} \quad (\text{A.3.7})$$

with

$$\mathcal{L}_{NLSM}^D = \frac{\Lambda^{D-2}}{2f_D} \sum_{\mu=1}^D \partial_\mu \vec{m} \cdot \partial_\mu \vec{m} \quad (\text{A.3.8})$$

The term f is the dimensionless coupling constant

$$f_D = \frac{c}{\rho_s} \Lambda^{D-2} \quad (\text{A.3.9})$$

For the nearest neighbor Heisenberg antiferromagnet we have [1]:

$$\Lambda = a^{-1} \quad (\text{A.3.10})$$

$$\rho_s = JS^2 a^{2-d} \quad (\text{A.3.11})$$

$$c_s = 2JSa d^{-1/2} \tag{A.3.12}$$

$$f = 2\sqrt{d}S^{-1} \tag{A.3.13}$$

It is easy to notice that the semiclassical limit (large S) corresponds to the weak coupling limit in the NLSM. In the absence of the topological term $\gamma[\vec{m}]$ the ground state of the quantum system is described by the classical energy of the NLSM in $d + 1$ dimensions.

Now we will investigate the role of the topological term in this kind of systems.

Appendix B

Topological term

It is known [8] that in one dimension the Berry phase is not vanishing and plays an important role in the physics of the system. The first term of the (A.3.7) *i.e.* the topological Berry phase is exactly $2\pi S Q_{xt}$, where Q_{xt} is the topological charge

$$Q_{xt} = \frac{1}{8\pi} \int dx dt \epsilon_{ij} \vec{m} \cdot (\partial_i \vec{m} \times \partial_j \vec{m}) \quad (\text{B.0.1})$$

Clearly when the spin S is an integer the contribution of this term in the action is irrelevant since $e^{2\pi S Q_{xt}} = +1$. If we assume compactified or periodic boundary conditions, the field $\vec{m}(x, t)$ is a map from the two dimensional sphere or torus to the sphere fixed by $|\vec{m}| = 1$. Thus Q_{xt} is an integer. On the other hand, when S is half-integer $e^{2\pi S Q_{xt}}$ can be both $+1$ or -1 , playing an important role in the quantum physics of the system. Haldane showed [8, 1] that because of this term, the integer spin chains are massive, while the half-integer chains are massless and then they fall in different universality classes. This is known as *Haldane's conjecture*.

In two space dimensions, consider the Néel vector $\vec{m}(x, y, t)$ with periodic boundary condition. We can in principle define a topological current J_μ

$$J_\mu = \frac{1}{8\pi} \epsilon_{\mu\nu\lambda} \epsilon_{a,b,c} m_a \partial^\nu m_b \partial^\lambda m_c \quad (\text{B.0.2})$$

If we consider the unit vector field $\vec{m}(x, y, t)$ well defined everywhere, the current does not change in time and we have a conserved charge

$$Q_{xy} = \int d^2x J^0(x, y, t) = \int d^2x \frac{1}{8\pi} \epsilon_{0\nu\lambda} \epsilon_{a,b,c} m_a \partial^\nu m_b \partial^\lambda m_c \quad (\text{B.0.3})$$

This is equal to the Pontryagin index [8] that one finds in $(1+1)D$, but now the time coordinate is substituted by the spacial coordinate y .

Wilczek and Zee [34] have defined a *skyrmion* of the associated σ model as a localized textural defect of the Néel field. Topologically distinct path of continuous vector field $\vec{m}(x, y, t)$ can be classified by the integer *Hopf* index H . In order to see if there is or not this Hopf term in the effective action of a $(2 + 1)D$ antiferromagnetic system we look at the Berry phase, under the assumption that the vector field $\vec{m}(x, y, t)$ is well-defined everywhere. Clearly, for a square lattice, this term is the sum along the y direction of all the Berry phases of the n chains of the square lattice that are $2\pi S Q_{xt}$. So the total Berry phase is [9]

$$\mathcal{S}_B = i2\pi S \sum_n (-1)^n Q_{xt}(y_n) \quad (\text{B.0.4})$$

Because of our assumptions, $\vec{m}(x, y, t)$ is continuous and the charges $Q_{xt}(y_n)$ are constant. For this reason the total sum vanishes and we conclude that there is no Hopf term for smooth configuration of the Néel field $\vec{m}(x, y, t)$ [9]. Moreover if $\vec{m}(x, y, t)$ is well defined everywhere, the Pontryagin index Q_{xy} is a constant of motion[9].

However is very important to notice that if this condition is relaxed, and than it is allowed to have tunnelling processes in which the charge Q_{xy} can change, the total Berry phase can assume value different from zero [9]. In that case there would be an intrinsic dependence of the system on the value of the spin S .

B.1 Without Berry phase

Ignoring the topological term in the action, the lattice model is simply a $O(3)$ quantum rotor, which fluctuations are well described by the $NL\sigma$ model. This means that exists a quantum phase transition at a critical point $g = g_c$ between an ordered ground state and a quantum paramagnetic ground state [27].

The ordered phase of the rotor model corresponds to a *Néel* ground state. This state clearly breaks the rotational symmetry because of the non vanishing value of the staggered magnetization [27]

$$\langle \hat{S}_i \rangle \sim \eta_i S \langle \vec{n}(x_i) \rangle = SN \hat{z} \quad (\text{B.1.1})$$

From numerical studies [27] we know that 2D quantum antiferromagnetic system with only nearest neighbour interaction J_1 has Néel order ground state for all value of spin S . Actually all of this system can be mapped into a rotor model with a value of g smaller than the critical value [27]. For spin equal $S = 1/2$ this g is find to be close to g_c .

It is also interesting to notice that it is possible to find system that are mapped onto a model with $g > g_c$, *i.e.* system that do not have Néel state as ground state. This is possible with frustration that is considering also the second neighbour interaction J_2 . For spin $S = 1/2$, several numerical studies have shown that for $J_2/J_1 = J_c \simeq 0.4$, the system loose his Néel order [27, 8]. It seems reasonable to identify this point with the critical one g_c . For $J_2/J_1 > J_c$ the rotational symmetry is restored and all the excitations are gapped [27, 8].

B.2 With Berry phase

As we have said before, Berry phase does not vanish for singular configuration. Considering a three component vector order parameter, the only admitted topological singularity is the *hedgehog*. This corresponds to a tunnelling event in which the Skyrmion number (B.0.3) changes. This is an integer for periodic boundary condition in space. Haldane in [9] describes pictorially this event: consider the configuration of $\vec{m}(x, y, t)$ with $Q = 1$ as an elastic sheet wrapped on a sphere. In principle the model is on a lattice, so the this can be visualized as a fine elastic mesh dividing the sphere into plaquettes. The mesh size is very small when there is a strong local Néel order. In this terms, a situation in which the area of one plaquette of the mesh becomes large enough to allow the sphere to pass through. Then, the mesh returns to be of a normal size. This corresponds to a tunnelling event in which Q_{xy} has changed from 1 to 0. In space-time this process are called *monopole* or *hedgehog* singularities of the vector field $\vec{m}(x, y, t)$.

Because of the periodic condition we cannot consider a single monopole event. We actually assume many of these processes such that $\sum_a \Delta Q = 0$, where the a label the plaquettes.

These events are the saddle points of the path integral of the lattice antiferromagnet [27]. They minimize the action and have a fourfold rotational symmetry about the plaquette a .

If there is a hedgehog centered in a point i of the space, the term $\mathcal{A}(i) \equiv \mathcal{A}[\vec{m}(i)]$ in Eq. (A.3.5) should support a $\pm 4\pi$ vortex singularity. For example one can take the configuration [27]:

$$\mathcal{A}(i) = 2 \sum_a Q_a \arctan\left(\frac{x_{i1} - X_{a1}}{x_{i2} - X_{a2}}\right) \quad (\text{B.2.1})$$

where $x_{i1,2}$ are the coordinate of the lattice site and X_a is the position of the center of the plaquette a . We have to evaluate the sum $\sum_i \mathcal{A}(i)$. In order to do this Haldane proposed to convert it in a sum over the plaquettes [9]. They are defined on the dual lattice and we can associate each plaquette with the site at its top right corner. One plaquette contributes to the Berry phase as $1/4$ times the sum of $\mathcal{A}(i)$ on the four corner sites.

Haldane shows [9] that the Berry phase factor can be written as

$$\prod_a (\zeta_a)^{2SQ_a} \quad (\text{B.2.2})$$

where the product is only on the singularities and Q_a can be ± 1 . The parameter ζ_a is $+1, i, -1$ or $-i$ and its value depends on the coordinate of the plaquette: it can be respectively (even,even) , (even,odd) , (odd, odd), (odd,even). Because of the fact that single hedgehogs are not allowed ($\sum_a Q_a = 0$), eq. (B.2.2) is invariant under translation of all the singularities and multiplication of ζ by a constant. From this formula we can see how the system behaves depending on the value of S . First notice that for even-integer spin the Berry phase factor is always equal to 1. This means that this kind of system can be seen exactly as a 3D classical Heisenberg model.

The eq. (B.2.2) shows us that configurations that differ only by a translation of a single hedgehog by one lattice spacing in the (10) or (01) direction, have the same amplitude but with different sign. This leads to a destructive interference for single hedgehogs [9].

Following the same procedure for *half-integer* spin, that are the most important for us, it is not difficult to see that there is a destructive interference between paths that differ by a shifting of the singularity in the directions (10) , (01) and (11). We can conclude that *hedgehods are quadrupled* and the disordered ground state, associated to a proliferation of this singularity, is fourfold degenerate [9].

In the first chapter it is shown how the proliferation of these topological singularities leads to a state call *spin-Peierls* or more commonly *valence-bond solid* (VBS).

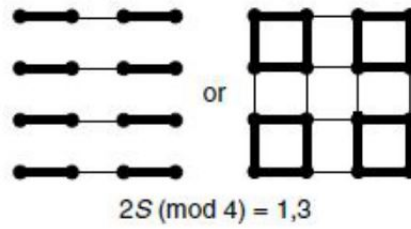


Figure B.1: The two possible configurations of the VBS state. From [27].

This state is characterized by the quantity [27]

$$P_{ij} = \langle \hat{S}_i \cdot \hat{S}_j \rangle \quad (\text{B.2.3})$$

This is in general invariant respect the group of the lattice symmetries. A VBS state is a state in which the value of P_{ij} breaks a lattice symmetry. In the $S = 1/2$ case for a square lattice, there are two possible patterns of the VBS order [30, 27]: P_{ij} line up in columns or plaquettes. These states, shown in Fig. B.1, clearly breaks the rotational symmetry and as we said before the ground state appears fourfold degenerate.

Appendix C

Monte Carlo tools

Monte Carlo methods are a class of computational algorithms based on random sampling. In fact the main idea of Monte Carlo simulation is to simulate the random thermal fluctuation of the system from state to state. In this simulations we follow the *time dependence* of a model that changes in a stochastic way depending on random numbers generated during the simulations [24].

Usually the main purpose of Monte Carlo simulations is to calculate the expectation value of some observable, for example the magnetization $\langle M \rangle$. In principle this correspond to the standard thermodynamic mean value [3, 24]

$$\langle M \rangle = \frac{\sum_{\mu} M_{\mu} e^{-\beta E_{\mu}}}{\sum_{\mu} e^{-\beta E_{\mu}}} \quad (\text{C.0.1})$$

where μ labels all the states of the system, β is $1/(K_B T)$ and E_{μ} is the energy of the state μ .

Clearly in numerical simulations a subset of these states μ is considered. Monte Carlo chooses this subset at random from a probability distribution p_{μ} [24]. Suppose to choose states μ_1, \dots, μ_N . Thus Eq. (C.0.1) become [24]

$$M_N = \frac{\sum_{i=1}^N e^{-\beta E_{\mu_i}} M_{\mu_i} / p_{\mu_i}}{\sum_{j=1}^N e^{-\beta E_{\mu_j}} / p_{\mu_j}} \quad (\text{C.0.2})$$

This value of M_N is called *estimator* of M and clearly it corresponds to $\langle M \rangle$ when $N \rightarrow \infty$ [24].

A simple choice for p_{μ} can be a uniform probability distribution: this is the so

called *simple sampling* [3] and (C.0.2) is simply

$$M_N = \frac{\sum_{i=1}^N e^{-\beta E_{\mu_i}} M_{\mu_i}}{\sum_{j=1}^N e^{-\beta E_{\mu_j}}} \quad (\text{C.0.3})$$

Clearly a more natural choice can be to take the probability distribution as $p_{\mu} \propto e^{-\beta E_{\mu}}$ [24]. In this case (C.0.1) simply becomes

$$M_N = \frac{1}{N} \sum_{i=1}^N M_{\mu_i} \quad (\text{C.0.4})$$

This is called *importance sampling*. In order to realise this kind of sampling *Metropolis et al.* in 1953 [18], proposed to construct a Markov process [3] where each state μ_{i+1} is constructed from the previous one μ_i with a transition probability $W(\mu_i \rightarrow \mu_{i+1})$. It was found [18] that it is possible to choose the transition probability W in such a way that, for $N \rightarrow \infty$, the function p_{μ_i} tends to the equilibrium distribution

$$p_{\mu_i}^{eq} = \frac{1}{Z} e^{-\beta E_{\mu_i}} \quad (\text{C.0.5})$$

where Z is the partition function. For these reasons, the transition probability has to be chosen in order to satisfy the relation [3]

$$p_{\mu_i}^{eq} W(\mu_i \rightarrow \mu_{i'}) = p_{\mu_{i'}}^{eq} W(\mu_{i'} \rightarrow \mu_i) \quad (\text{C.0.6})$$

Thus the ratio of transition probabilities depends only on the difference of the energies of the two states.

$$\frac{W(\mu_i \rightarrow \mu_{i'})}{W(\mu_{i'} \rightarrow \mu_i)} = e^{-\beta(E_{\mu_{i'}} - E_{\mu_i})} \quad (\text{C.0.7})$$

A suitable choice of W is the so called *Metropolis form*

$$W(\mu_i \rightarrow \mu_{i'}) = \tau_0^{-1} \exp(-\beta \Delta E) \quad \Delta E > 0 \quad (\text{C.0.8})$$

$$= \tau_0^{-1} \quad \Delta E < 0 \quad (\text{C.0.9})$$

where $\Delta E = E_{\mu_{i'}} - E_{\mu_i}$ and τ_0 is an arbitrary factor, that is usually chosen as a unit of "Monte carlo time", well described below.

In our specific simulations we have a three dimensional lattice of finite size L . At each site we consider a unit three dimensional vector *i.e.* the spin. A configuration is uniquely defined once we know the direction of each vector. A new configuration is

constructed by the previous one by changing a direction of a single spin. The choice of the spin and of its new direction is totally random. In particular the direction is selected by choosing at random the two polar angles θ and ϕ . A uniform distribution of these angles on the S_2 sphere is obtained by taking [33]

- $\phi = 2\pi u$
- $\cos^{-1}(2\nu - 1)$

where u and ν are random variates on the interval $(0, 1)$.

The *single-flip Metropolis algorithm* for our models is characterized by

- choose a random spin of the system
- choose a random new direction for that spin
- compute the difference of energy ΔE between the two configurations
- accept the new configuration with a probability given by $e^{-\frac{\Delta E}{T}}$

It's easy to see that if the new configuration has an energy lower than the old, the exponential is greater than one and this means that we always have to accept it.

The repetition of this procedure $L \times L \times L$ times forms a *Monte Carlo sweep* (MCS), that represents our "Monte Carlo time" t . For each of MCS we take a value of some observable that we are looking for and then we take the mean value

$$\langle M \rangle = \frac{1}{N_{MCS}} \sum_{t=1}^{N_{MCS}} M_t \quad (\text{C.0.10})$$

C.1 Statistical error

Here we will briefly talk about the statistical error associated to Monte Carlo sampling. Suppose to have N observations of M_μ , $\mu = 1, \dots, N$. Thus the square of statistical error is [24, 3]

$$\langle (\delta M)^2 \rangle = \left\langle \left[\frac{1}{N} \sum_{\mu=1}^N (M_\mu - \langle M \rangle) \right]^2 \right\rangle = \quad (\text{C.1.1})$$

$$\langle (\delta M)^2 \rangle = \left\langle \left[\frac{1}{N} \sum_{\mu=1}^N (M_\mu - \langle M \rangle) \right]^2 \right\rangle \quad (\text{C.1.2})$$

$$= \frac{1}{N^2} \sum_{\mu=1}^N \langle (M_\mu - \langle M \rangle)^2 \rangle + \frac{2}{N} \sum_{\mu_1=1}^N \sum_{\mu_2=\mu_1+1}^N \left(\langle M_{\mu_1} M_{\mu_2} \rangle - \langle M \rangle^2 \right) \quad (\text{C.1.3})$$

Now defining a time $t_\mu = \delta t \mu$, where δt is the time interval between two observations M_μ and $M_{\mu+1}$. Then changing μ_2 to $\mu_2 + \mu$ and transforming the summation into a time integration, we have [3, 21]

$$\langle (\delta M)^2 \rangle = \frac{1}{N} \left(\langle M^2 \rangle - \langle M \rangle^2 \right) \left[1 + \frac{2}{\delta t} \int_0^{t_0} \left(1 - \frac{t}{t_n} \right) \frac{\langle M(0)M(t) \rangle - \langle M \rangle^2}{\langle M^2 \rangle - \langle M \rangle^2} dt \right] \quad (\text{C.1.4})$$

Defining the *autocorrelation function* [24, 3, 15]

$$\phi_M(t) = \frac{\langle M(0)M(t) \rangle - \langle M \rangle^2}{\langle M^2 \rangle - \langle M \rangle^2} \quad (\text{C.1.5})$$

and the *autocorrelation time*

$$\tau_M = \int_0^\infty \phi_M(t) dt \quad (\text{C.1.6})$$

we are able to write [3]

$$\langle (\delta M)^2 \rangle = \frac{1}{N} \left[\langle M^2 \rangle - \langle M \rangle^2 \right] \left(1 + 2 \frac{\tau_M}{\delta t} \right) \quad (\text{C.1.7})$$

where it was considered $t \ll tn$. If we take $\delta t \ll \tau_M$ we find

$$\sigma = \sqrt{\langle (\delta M)^2 \rangle} \simeq \sqrt{\frac{2\tau_M}{N\delta t} \left[\langle M^2 \rangle - \langle M \rangle^2 \right]} \quad (\text{C.1.8})$$

The autocorrelation function for the Classical $O(3)$ Heisenberg system of size $L = 8$ is shown in Fig. C.1 at $T = 1.2$. As we can see the function zero after a Monte Carlo time about 20 MCSs. This is the time that we have to wait in order to have a measure independent of the previous one. We expect an autocorrelation time $2\tau \simeq 20$. Knowing that [24, 15] $\phi_M \sim e^{-t/\tau_M}$ we have that τ_M is the slop of the straight line in the Fig. C.2 . We actually found $\tau_0 = 9$ as expected.

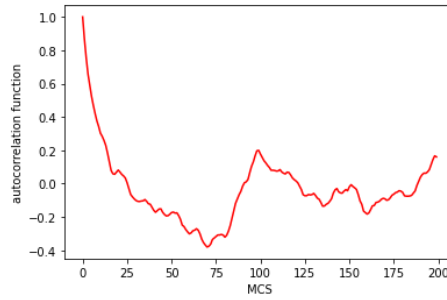


Figure C.1: Autocorrelation function ϕ_M . It's easy to see that the function reach the zero after about 20 MCSs.

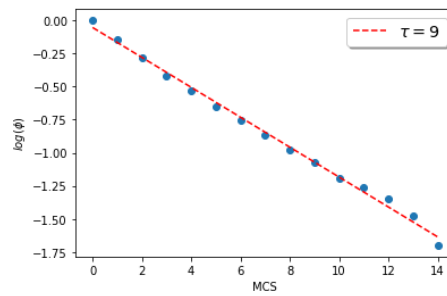


Figure C.2: Semi-log plot of the logarithm of ϕ_M as a function of the MCSs.

Bibliography

- [1] A. AUERBACH, *Interacting electrons and quantum magnetism* (Springer-Verlag) (1994);
- [2] B. BERG, M. LUSCHER, Nucl. Phys. **B190**, [FS3] 412 (1981);
- [3] K. BINDER, D. W. HEERMANN, *Monte Carlo Simulation in Statistical Physics: an introduction* (Springer) (2019);
- [4] P. M. CHAIKIN, T. C. LUBENSKY, *Principles of condensed matter physics* (Cambridge University Press) (1995);
- [5] S. CHAKRAVARTY, B. I. HALPERIN, D. R. NELSON, Phys. Rev. B **39**, 2344 (1989);
- [6] P. COLEMAN, C. PÉPIN, Q. SI, J. RAMAZASHVILI, Phys. Condens. Matt. **13**, 723 (2001);
- [7] J. M. CARMONA, A. PELISSETTO, E. VICARI, Phys. Rev. B **61**, 15136 (2000);
- [8] E. FRADKIN, *Field theories of condensed matter physics* (Cambridge University Press) (2013);
- [9] F. D. M. HALDANE, Phys. Rev. Lett. **61**, 1029 (1988);
- [10] C. HOLM, W. JANKE, Phys. Rev. B **48**, 936 (1993);
- [11] C. ITZYKSON, J. M. DROUFFE, *Statistical field theory - volume 1* (Cambridge University Press) (1989);
- [12] J. V. JOSÉ, L. P. KADANOFF, S. KIRKPATRICK, D. R. NELSON, Phys. Rev. B **16**, 1217 (1977);

- [13] M. KAMAL, G. MURTHY, Phys. Rev. Lett. 71, 1911 (1993);
- [14] L. D. LANDAU, E. M. LIFSHITZ, E. M. PITAEVSKII, *Statistical Physics* (Butterworth-Heinemann, New York) (1999);
- [15] D. P. LANDAU, K. BINDER, *A Guide to Monte Carlo Simulations in Statistical Physics* (Cambridge University Press) (2021);
- [16] M. LAU, C. DASGUPTA, Phys. Rev. B **39**, 7212 (1989);
- [17] S. MA, *Modern Theory of Critical Phenomena* (W.A. Benjamin) (1976);
- [18] N. METROPOLIS, A. W. ROSENBLUTH, M.N. ROSENBLUTH, A. H. TELLER, E. TELLER, J. Chem. Phys. **21**, 1087 (1953);
- [19] O. MOTRUNICH, A. VISHWANATH, cond-mat/0311222 (2004);
- [20] M. MORANDI, *The Role of Topology in Classical and Quantum Physics* (Springer-Verlag) (1992);
- [21] H. MULLER-KRUMBHAAR, K. BINDER J. Stat. Phys. **8**, 1 (1973);
- [22] G. MURTHY, S. SACHDEV Nucl. Phys. B **344**, 557 (1990);
- [23] M. E. MUSSARDO, G. *Statistical field theory: an introduction to exactly solved models in statistical physics* (Oxford University Press, Oxford) (2010);
- [24] M. E. NEWMAN, G. T. BARKEMA, *Monte Carlo Methods in Statistical Physics* (Oxford University Press, Oxford) (1999);
- [25] A. PERELOMOV, *Generalized Coherent States and Their Applications* (Springer) (1986);
- [26] N. READ, S. SACHDEV, Phys. Rev. Lett. B **62**, 1694 (1989);
- [27] S. SACHDEV, *Quantum phase transitions* (Cambridge University Press) (2011);
- [28] S. SACHDEV, *Quantum phases and phase transitions of Mott insulators* (Schollwöck U., Richter J., Farnell D.J.J., Bishop R.F.) Quantum Magnetism. Lecture Notes in Physics, vol 645. (Springer, Berlin, Heidelberg) (2004);

- [29] T. SENTHIL, A. VISHWANATH, L. BALENTS, S. SACHDEV, P. A. FISHER, *Science* **303**, 1490 (2004);
- [30] T. SENTHIL, A. VISHWANATH, L. BALENTS, S. SACHDEV, P. A. FISHER, *Phys. Rev. B* **70**, 144407 (2004);
- [31] T. SENTHIL, A. VISHWANATH, L. BALENTS, S. SACHDEV, P. A. FISHER, *J. Phys. Soc. Japan*, **70**, p. 1 (2005);
- [32] J. VILLAIN, *J. Phys. (Paris)*, **36**, 581 (1975);
- [33] WEISSTEIN, E. W. *Sphere Point Picking*, From *MathWorld-A Wolfram Web Resource*, accessed 2 September 2021, <https://mathworld.wolfram.com/SpherePointPicking.html>;
- [34] F. WILCZEK, A. ZEE *Phys. Rev. Lett.* **51**, 2250 (1983);
- [35] K.G. WILSON, J. KOGUT, *Phys. Rep. B* **12**, 75 (1974);